CALCULATIONS OF EXTINCTION ANGLES AND REFRACTIVE INDICES BY MEANS OF A STEREONET

BY

KATHERINE L. SPRINGER
THE OHIO STATE UNIVERSITY

A SENIOR THESIS SUBMITTED
TO FULFILL THE REQUIREMENTS
FOR THE B.S. IN GEOLOGY 1984

THESIS ADVISOR

Ernest G. Ehlers

DEPARTMENT OF GEOLOGY
AND MINERALOGY

TABLE OF CONTENTS

LIST OF ILLUSTRATIONS

LIST OF TABLES

RESULTS

INTRODUCTION

The speed with which light travels through a mineral is dependent upon its density. A dense mineral contains a larger number of atoms per unit volume than a less dense mineral. Light must interact with a relatively larger number of atoms and the velocity is decreased.

A light ray travels at different speeds for different directons of vibration in most minerals; such minerals are termed anisotropic. If an anisotropic grain is viewed in transmitted light with a polarizing microscope, the orientation of the grain on the stage will determine which of its indices of refraction may be measured. The index of refraction (λ) is related to the velocity of light within a substance (by the relationship $\lambda = 1/V$, where V equals velocity). The faster the ray travels through the mineral, the smaller the index of refraction.

Uniaxial crystals show one unique crystallographic direction and have only a single optic axis. Biaxial crystals show two directions of uniform light velocity (optic axes) and belong to one of three systems: orthorhombic, monoclinic or triclinic. Materials within each of these three crystal systems have three principal indices of refraction α , β , and γ . It is in biaxial crystals that there are three corresponding principal vibration directions: X, Y, and Z, which are named the principal vibration directions.

The vibration directions X, Y, and Z are the directions along which the refractive indices α , β , γ are measured. Intermediate directions permit measurement of intermediate indices. Directions between X and Y or Y and Z permit measurement of α' or γ' , respectively. These prime values may be determined by calculations from data plotted on a stereonet.

THE STEREONET

In representations of the geometric relations between crystallographic directions and optical properties, stereographic projections are commonly used. The stereonet in Figure 1 is used to plot three dimensional crystals on a two dimensional plane surface. Circles of maximum diameter are termed great circles and the outer circle is designated the primitive circle. Circles of less than maximum diameter are termed small circles. Crystal faces are represented on the sphere as great circles. Plotting of points on the stereographic net permits measurements of angles between various directions in the crystal. In addition, projections can be rotated into any position desired. Such rotations are facilitated by placing tracing paper over the center of the net. Commonly, a tack is placed in the center of the projection to hold the paper and permit rotation during measurement.

FRESNEL'S LAW

Vibration directions may be precisely located in a crystal by a rule postulated by Fresnel in 1928. This rule is based upon the location of the optic axes and the wave normal directions.

Figure 2 explains the rule. Given the wave normal OW and the two optic axes OA and OB, the vibration directions WN and Wn associated with wave normal can be located as follows: Construct planes containing OA and OW, and OB and OW (shaded). The vibration directions WN and Wn lie in the unshaded planes that bisect the angle between the shaded planes. Since the line of intersection of the vibration planes WN and Wn correspond to OW, their precise direction is known (Bloss, 1961).

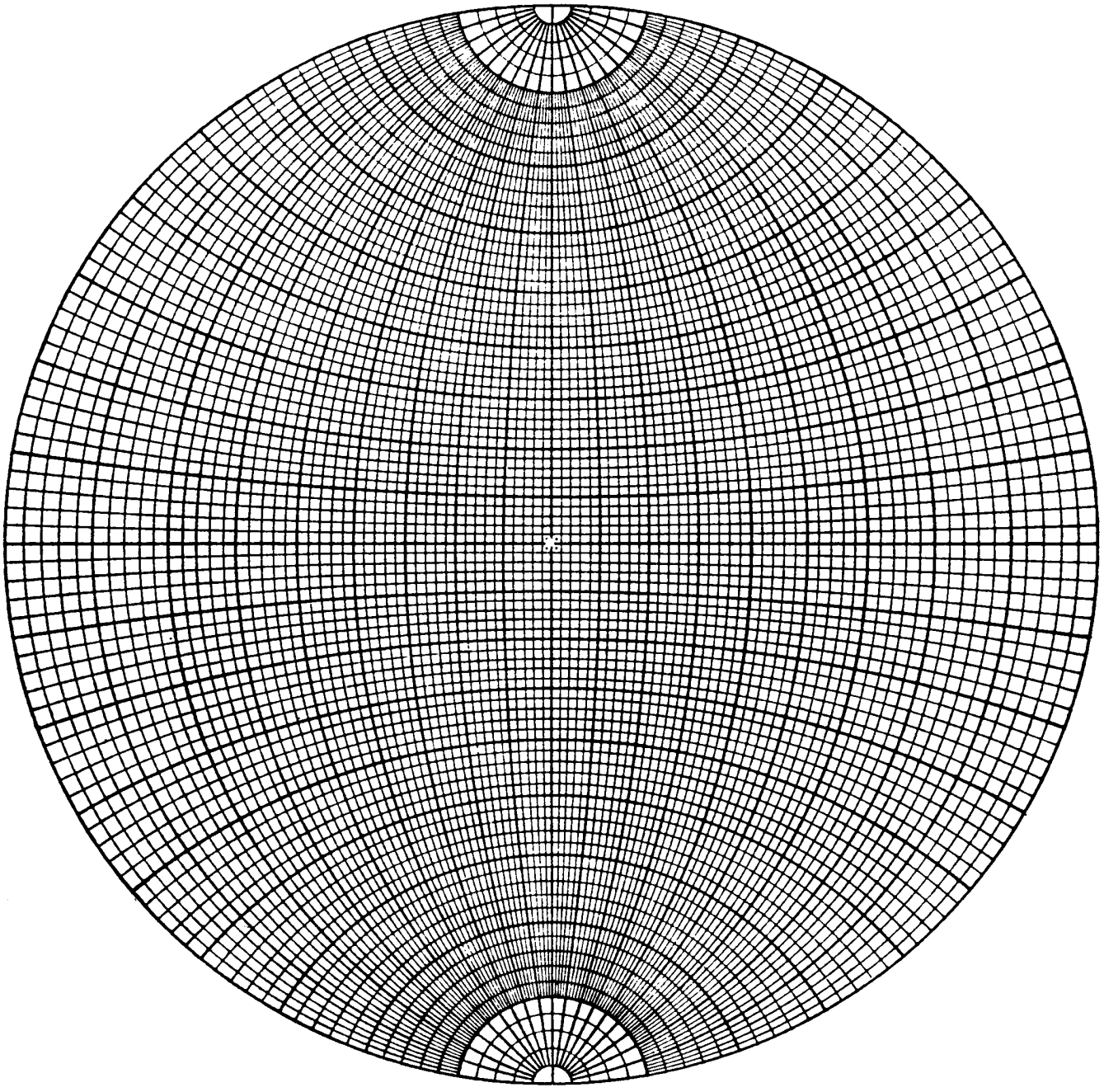

Figure 1. The Stereonet

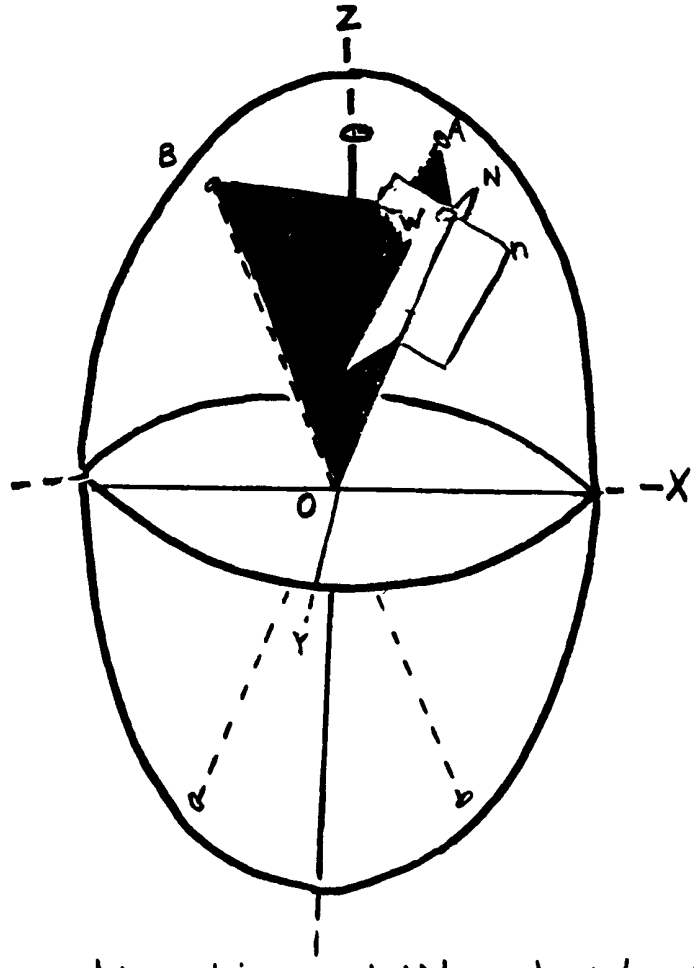

The vibration directions WN and Wn, that are associated with wave normal OW, as obtained by the Biot-Fresnel rule

Figure 2. Fresnel's Law illustrated (Bloss, 1961)

PLOTTING ON THE NET - SYSTEMS

An orthorhombic mineral's crystallographic axes a, b and c correspond in one of six different ways to the optical directions X, Y and Z. The mineral's crystallographic axes are plotted on the net with the +a axis on the south side of primitive circle. The (-) end of the a axis is correspondingly placed at the north pole on the net 180° from the positive end. The positive end of the b axis is plotted on the east side of the primitive circle, and -b is 180° away on the west side. The (+) end of the c axis is plotted in the center. In Figure 3A, the axes are set up as shown in an orthorhombic crystal. In Figure 4, the axes are plotted on the net.

There is a change in the orientation of a monoclinic mineral (Figure 3B). In a monoclinic mineral, one optic direction (X, Y or Z) is parallel to the b crystallographic axis and the other two lie in the ac crystallographic plane of symmetry (010). There are three possible orientations: X=b, Y=b, or Z=b. In the ac plane perpendicular to b, the remaining two optic directions (i.e. also the indices) lie at some angle to a or c crystallographic axes and are usually expressed as c∧X, c∧Y, or c∧Z (Figure 5).

The b axis is placed on the net in the same way as in orthorhombic minerals, in the east-west direction. The axes a and c are plotted along the vertical N-S plane (with c at the center of the net) 90° apart (Figure 6). Only the crystal axis b will necessarily be X, Y or Z.

The (+) crystal axis a is on the underside of the net, as in B, the a∧c angle is always greater than 90° (Figure 3B).

The triclinic system has an oblique relationship between a, b, c and X, Y, Z (Figure 3C) and is not covered here.

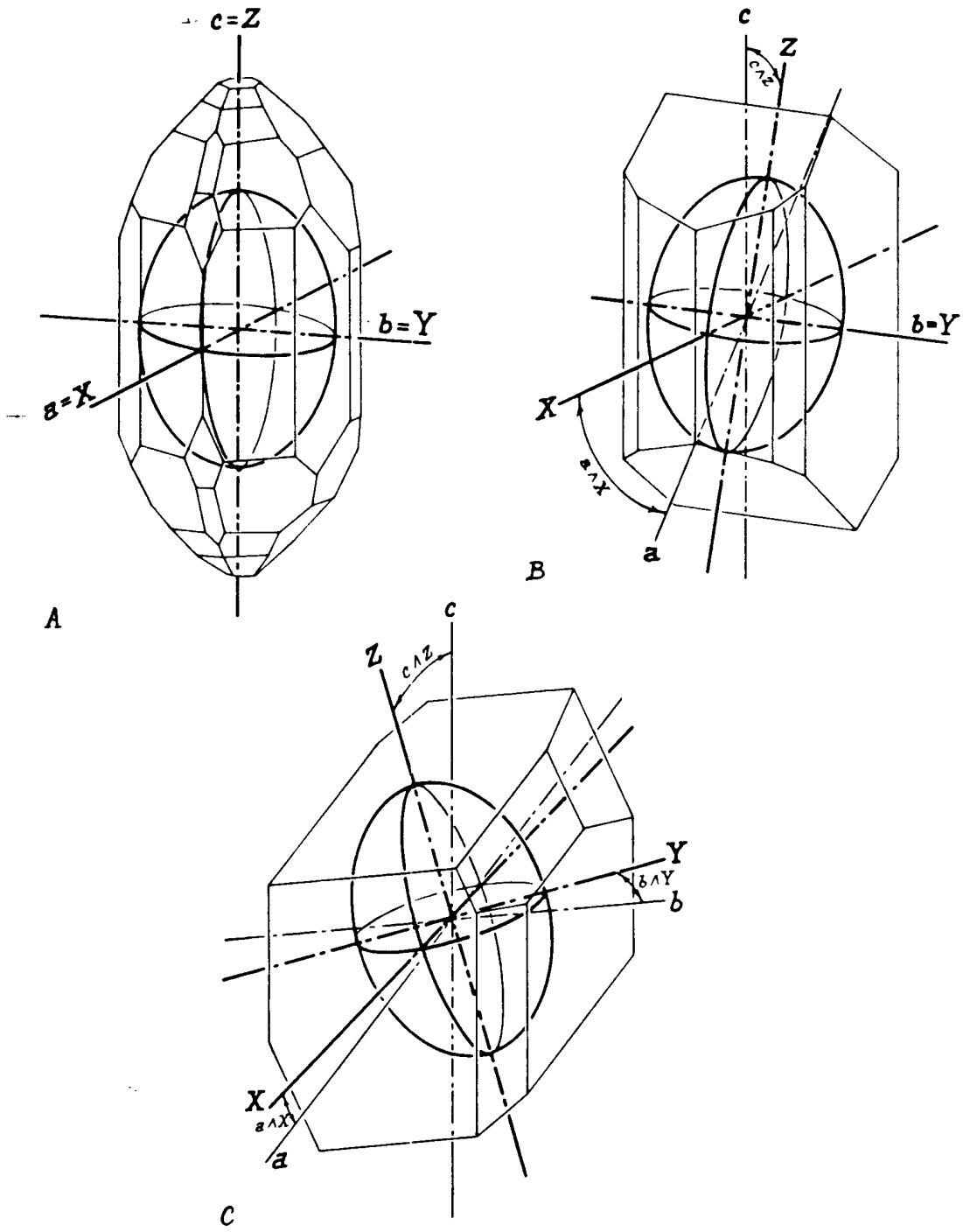

Figure 3. Crystallographic Axes in the Three Systems

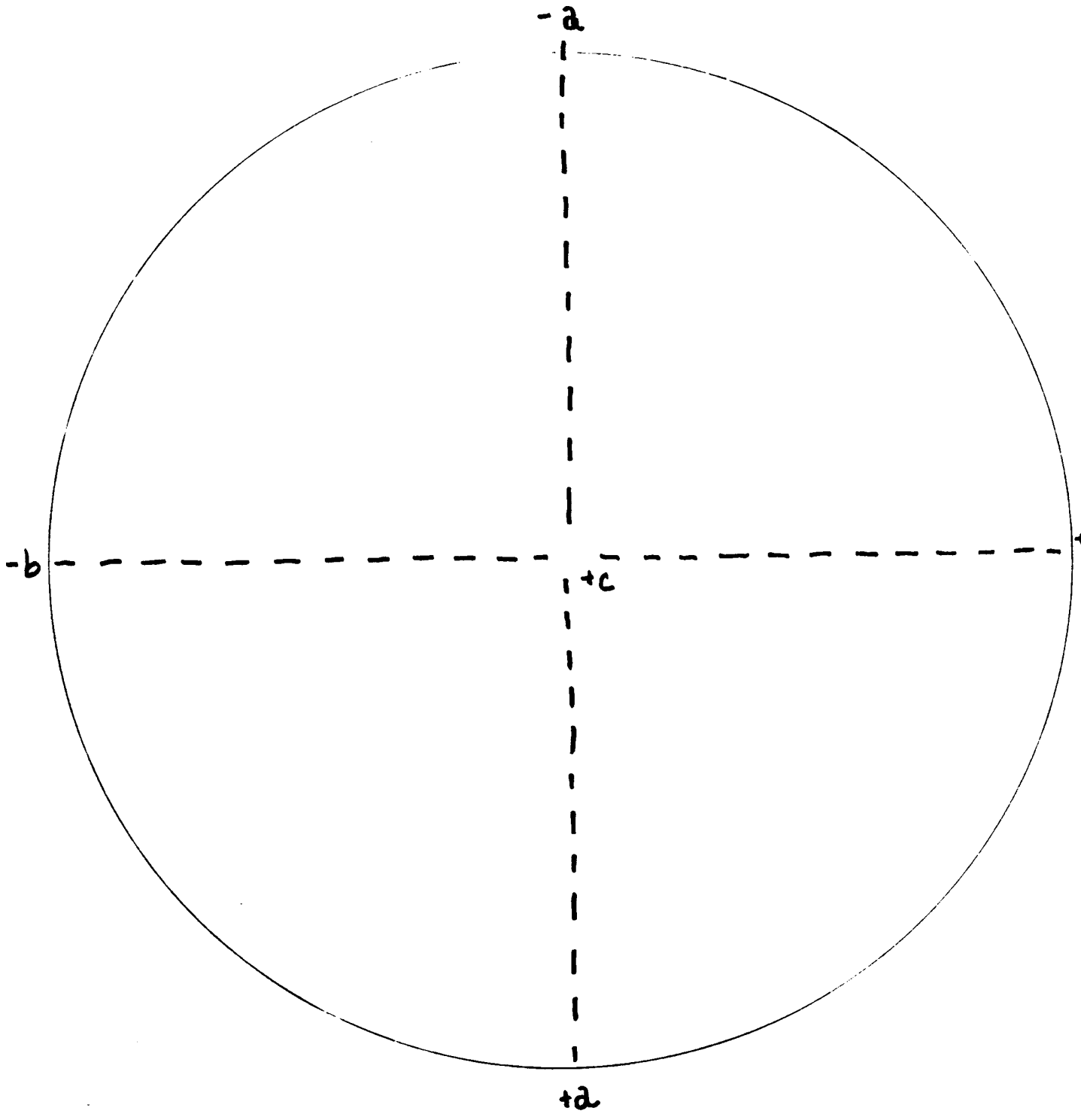

Figure 4. Placement of Crystallographic Axes in an Orthorhombic System on a Stereonet

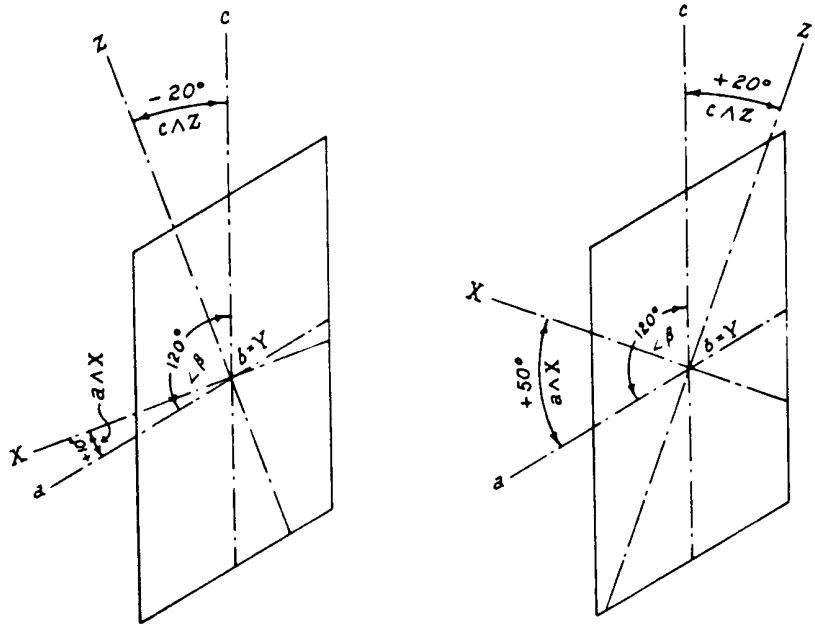

Figure 5. Placement of Crystallographic Axes in a Monoclinic System on a Grain

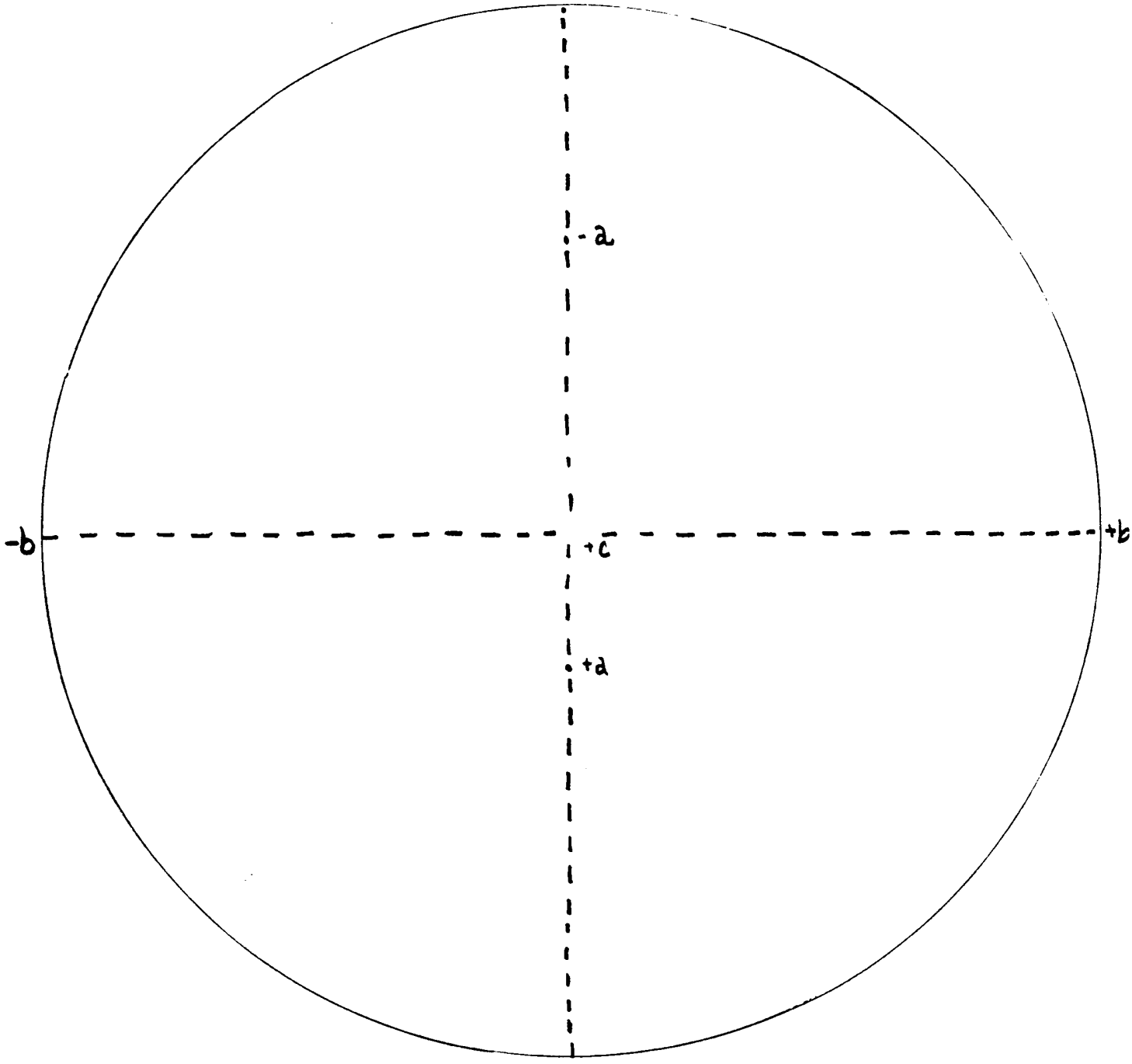

Figure 6. Placement of Crystallographic Axes in a Monoclinic System on a Stereonet

PROCEDURE

Turning to specific minerals mainly in the monoclinic system, the procedure for plotting on the net is demonstrated.

The first pertinent information needed is which of the three principal optic directions, X, Y, or Z, corresponds to the b crystallographic axis. If b=Y, Z and X must be plotted along the N-S (ac) vertical plane. If the angle measured from the c crystallographic axis is given as $c \wedge Z = -20°$, Z on the net in the -a direction, as shown in Figure 7. (Angles are measured in 2° intervals.)

If $c \wedge Z$ is positive, the optic direction X is plotted to the south (toward +a). If no sign is attached to the direction, it is assumed to be positive. After this vibration direction is plotted, the third principal index (Figure 8) is plotted at 90° within the ac plane.

The optic angle (2V) is the angle between the optic axes. The vibration direction bisecting the larger angle between the optic axes is designated as the obtuse bisectrix or BX_o. The vibration direction bisecting the smaller angle between the two optic axes is the BX_a or acute bisectrix. If the optic sign is positive, the acute angle is bisected by Z. If the optic sign is negative, the acute angle is bisected by X. Note that BX_a, BX_o and the two optic axes lie in the same plane.

The ϕ and ρ coordinates for a given face may be plotted on the net and are given in terms of the face normal. This face normal is perpendicular to the face itself, and it is placed in square brackets (i.e. [010]). The ρ angle is the angular distance from the c axis. The ϕ angle is the horizontal angular distance measured from the positive end of the b axis.

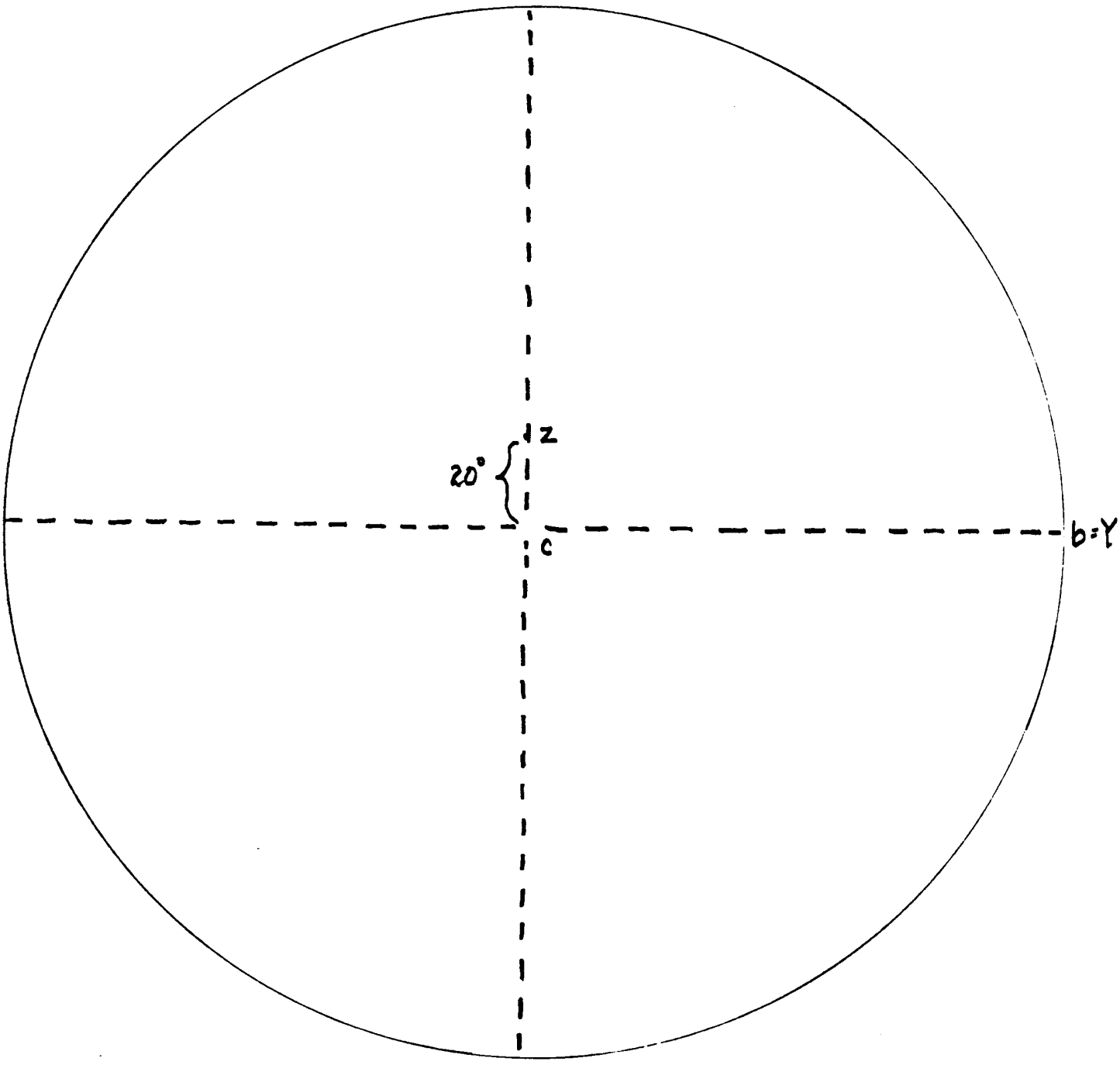

Figure 7. Plot of Second Crystallographic Axis, Angle C∧ Z on the Stereonet

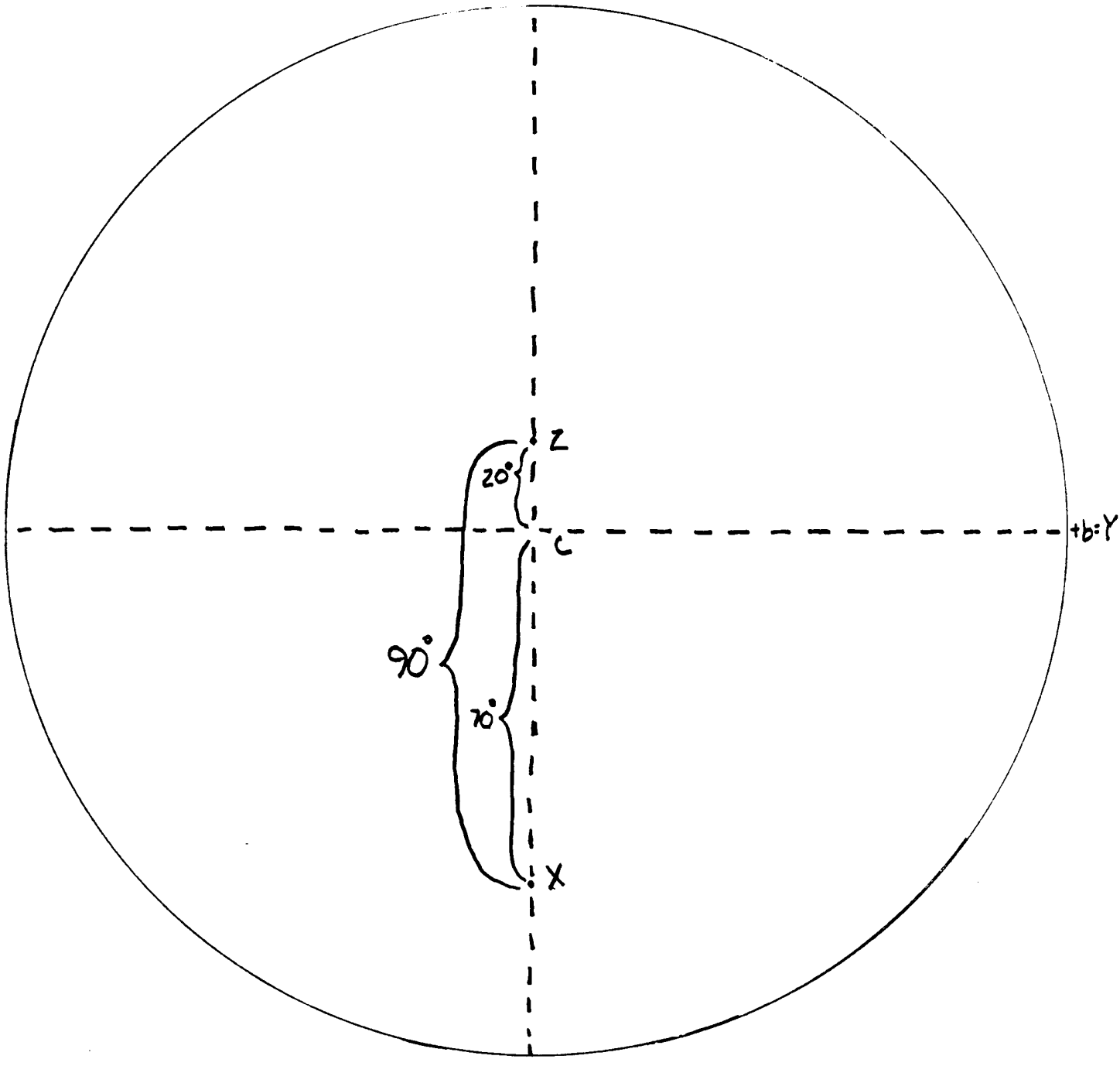

Figure 8. Placement of the Third Principal Optic Direction on a Stereonet of a Monoclinic Mineral

If ϕ is positive, it is measured in a southerly direction. Figure 9 has a plot of the face normal [110] when ρ =90° and ϕ =43.5°. The great circle representing the face (110) is plotted 90° away from [110] (Figure 10).

Fresnel's Law uses the face normal and the optic axes positions to find the vibration directions. The vibration directions are planes which include the face normal. Two great circles may be drawn through the face normal and each of the plotted positions of optic axes. The midpoint between these two points (along the line which represents the crystal face (i.e. the stage)) is one of the extinction positions. The other extinction position is 90° away from that point on the same great circle (Figure 11).

If these extinction positions do not correspond to α , β or γ , then they must be the intermediate values α' or γ' . These values are assigned α' if closer to α than γ , and γ' if closer to γ than α .

These two positions also represent the extinction positions for that particular cleavage surface. To measure the extinction angle for a particular cleavage face, measure from that face (if plotted on the net) to an adjacent intersecting cleavage surface.

This second cleavage face is plotted on the net as the face normal $[1\bar{1}0]$, and the corresponding face is plotted 90° away from this point along a great circle. The extinction angle in this case is 25° (Figure 12).

The angle is measured from the second cleavage face to the extinction position. The measurement must be taken from the intersection of the cleavage face and the stage, and the angle itself is usually described in terms

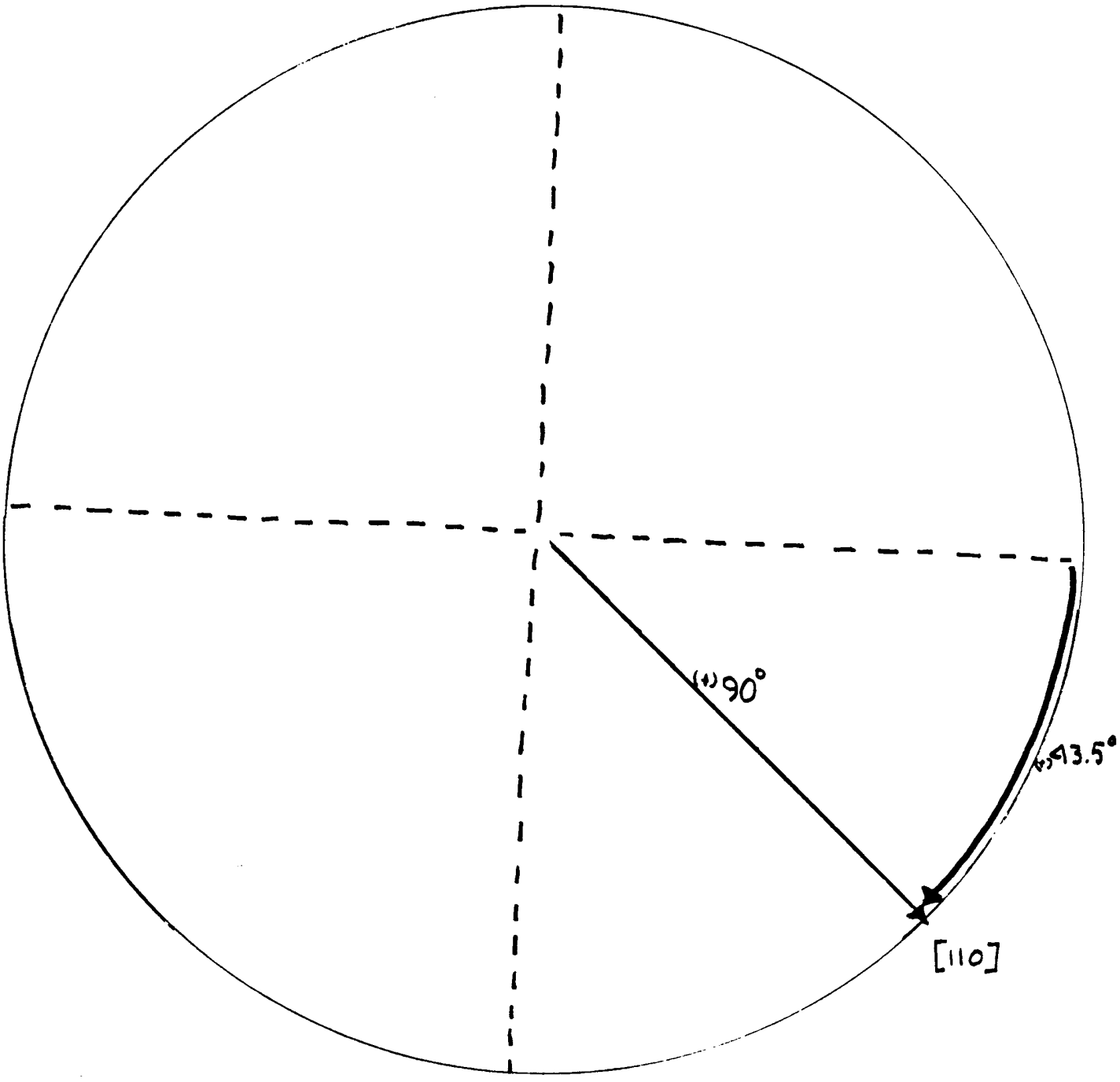

Figure 9. Orientation of a Mineral in Terms of ϕ and ρ Coordinates, and Their Corresponding Placement on the Stereonet

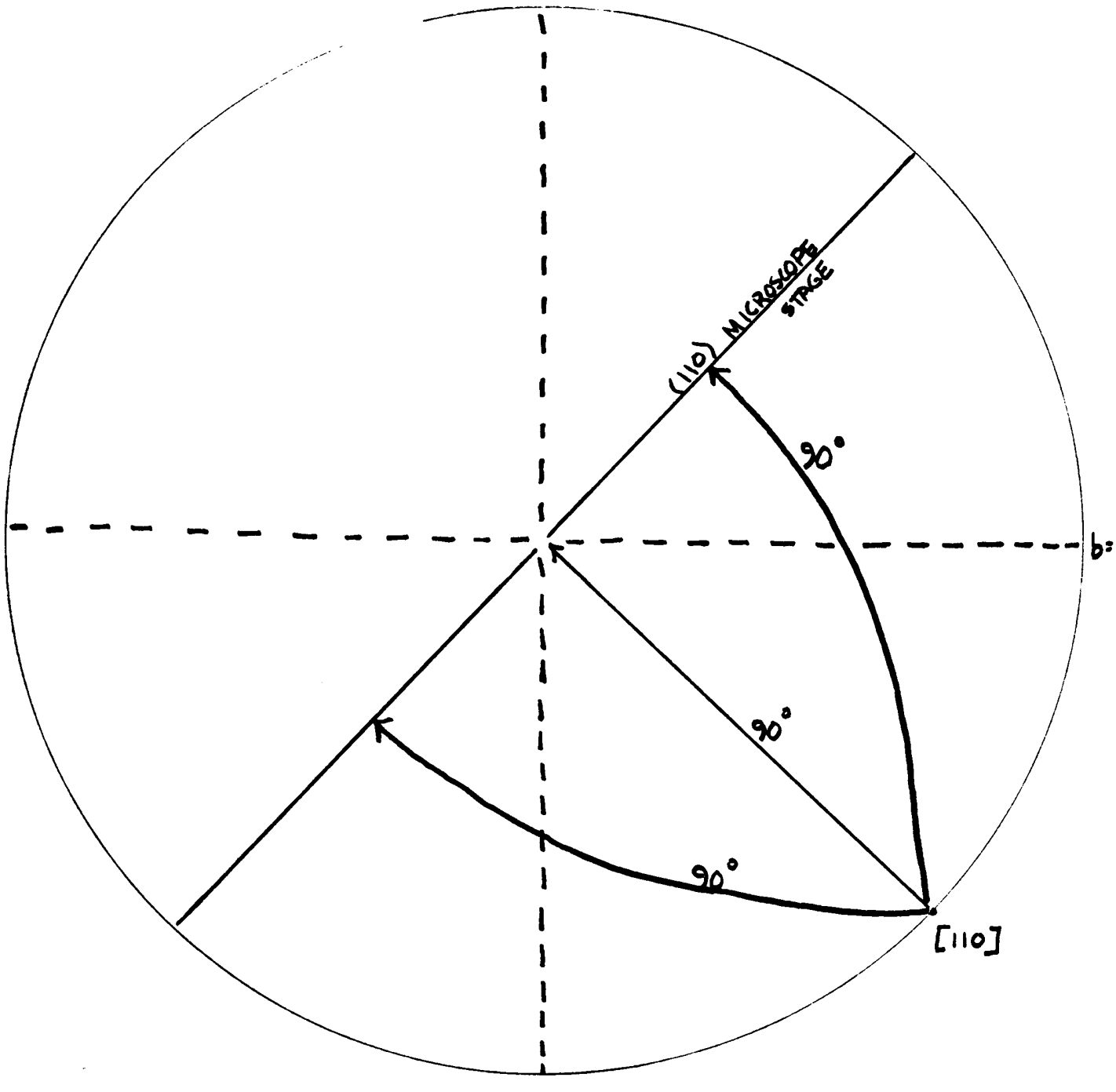

Figure 10. Plotting the Face Normal and Its Corresponding Face, in Addition to the Optic Axes as Plotted on a Stereonet

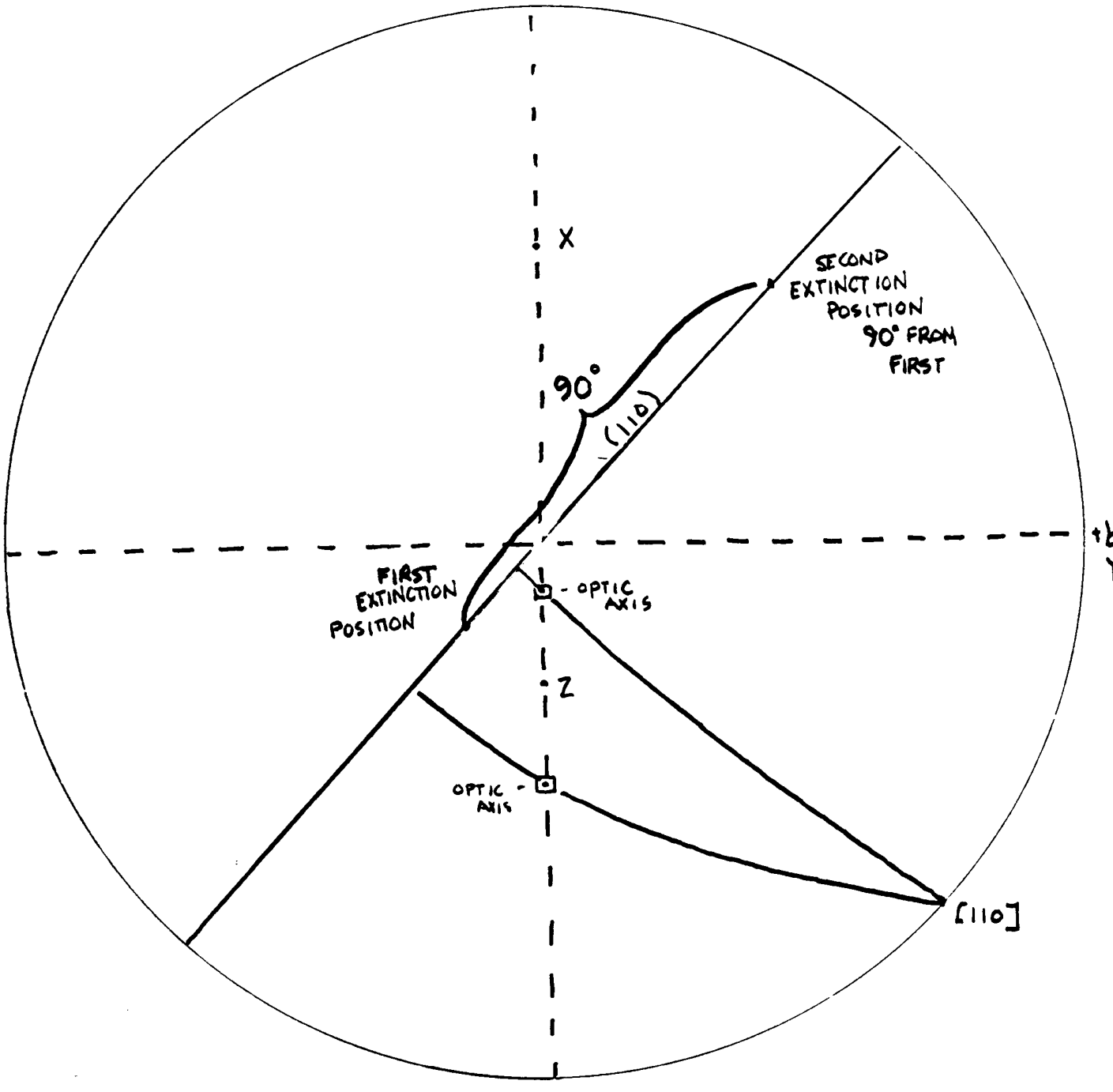

Figure 11. The Location of the Extinction Positions on a Stereonet

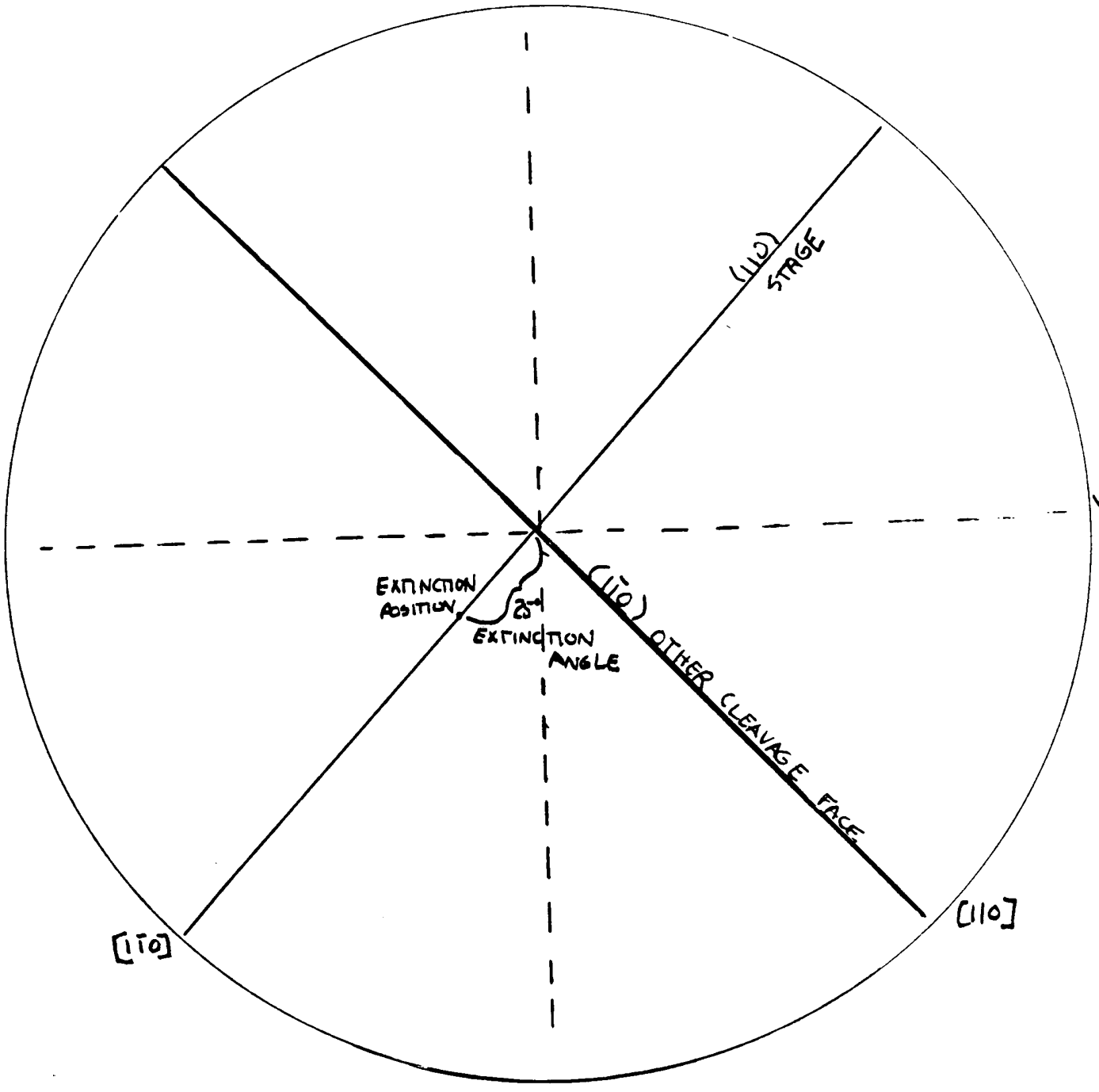

Figure 12. Measurement of the Extinction Angle with a Second Cleavage Face, Both as Plotted on the Stereonet, and as a Grain on the Microscope Stage

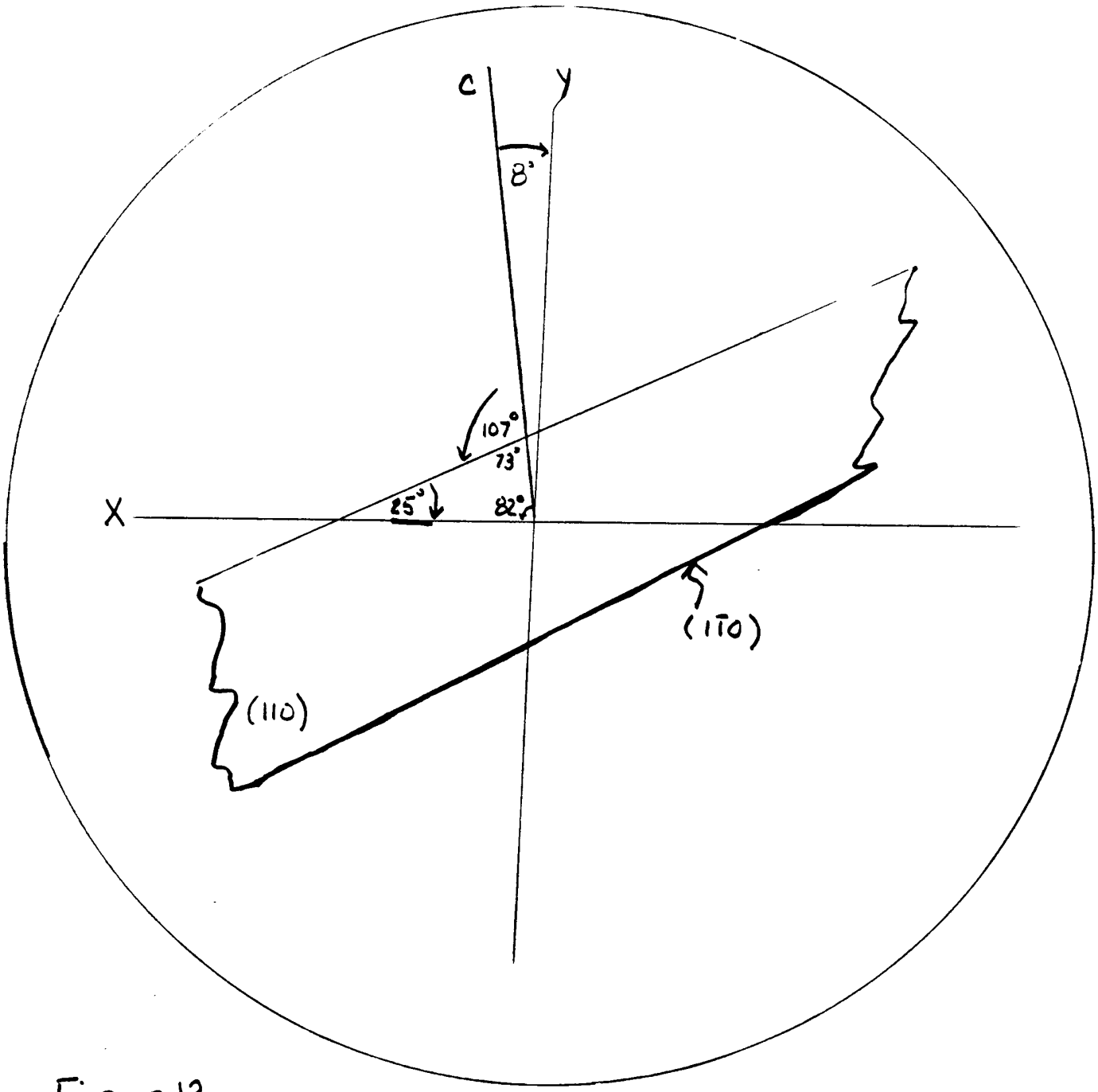

Figure 12.
Grain lying on (110) surface. The angle c∧x is 82°. The angle between c and (1$\bar{1}$0) is 73°. The angle of x∧(1$\bar{1}$0) is 25°, or the extinction angle for the fragment.

of the larger index. This method may be utilized for all biaxial minerals, and permits measurements of extinction angles for any other cleavage face plotted on the net.

In order to locate the index values, the optic triangle is drawn. This is the triangle connecting X, Y and Z along great circles. If the extinction positions falls within this triangle, one may measure the ρ and ϕ angles of α' or γ' on the net. In the case of the optic triangle in Figure 13, ρ is the angle measured from the extinction position to γ along a great circle, and is measured from α' along the $\alpha\beta$ great circle to the position of X(α).

This information is substituted into the equation for the biaxial indicatrix (Wahlstrom, 1951).

$$\frac{X^2}{\alpha^2} + \frac{Y^2}{\beta^2} + \frac{Z^2}{\gamma^2} = 1$$

This equation, in rectangular coordinates, permits the values α' and γ' to be calculated. In Figure 14, OP equals the randomly directed radius of a biaxial indicatrix.

The length OP may be calculated. The length OP corresponds to either α' or γ' (depending upon its position). The equation used is:

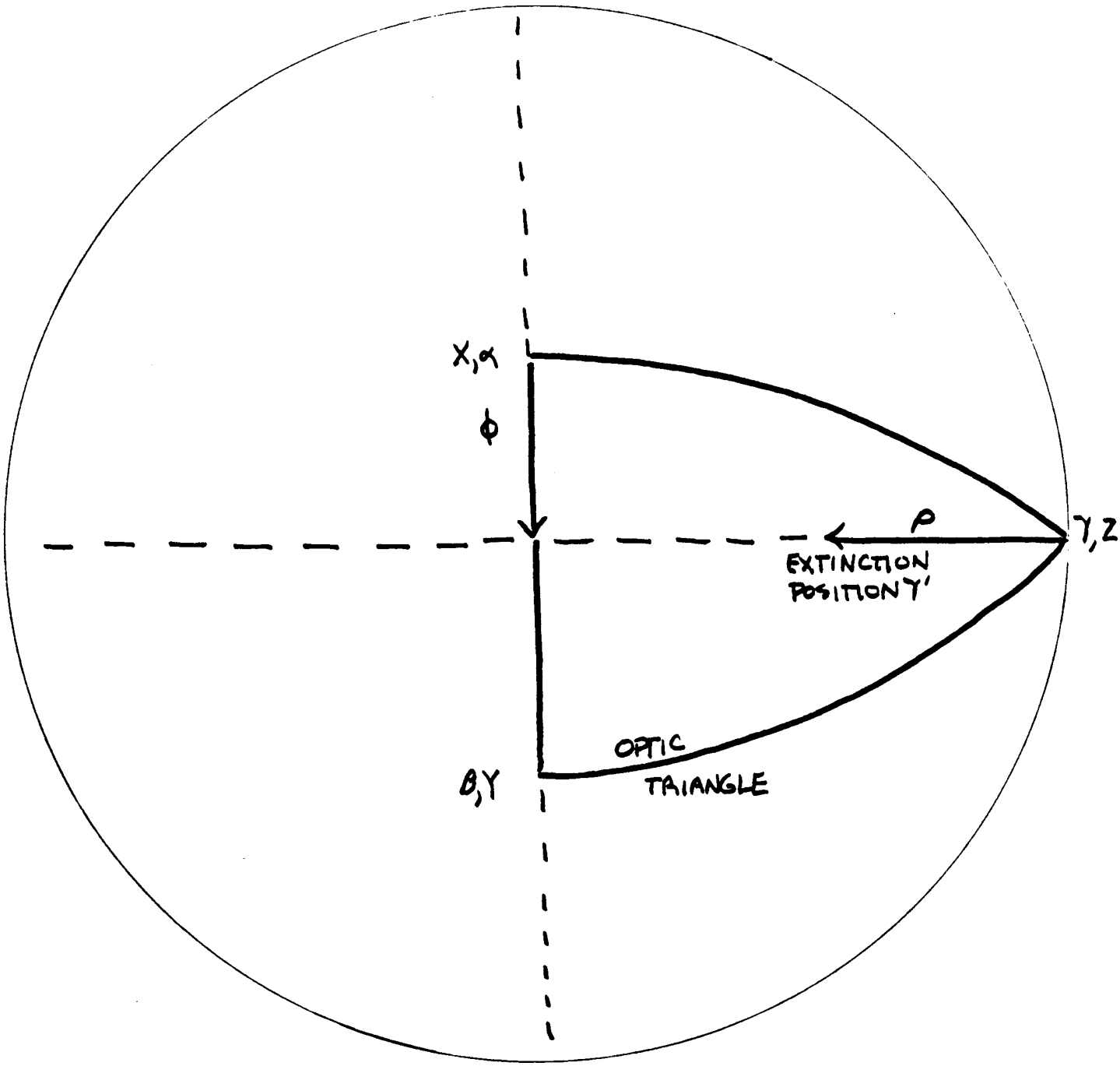

Figure 13. The Optic Triangle as Drawn on the Stereonet

ϕ and ρ are stereographic coordinates that orient line OP in the indicatrix

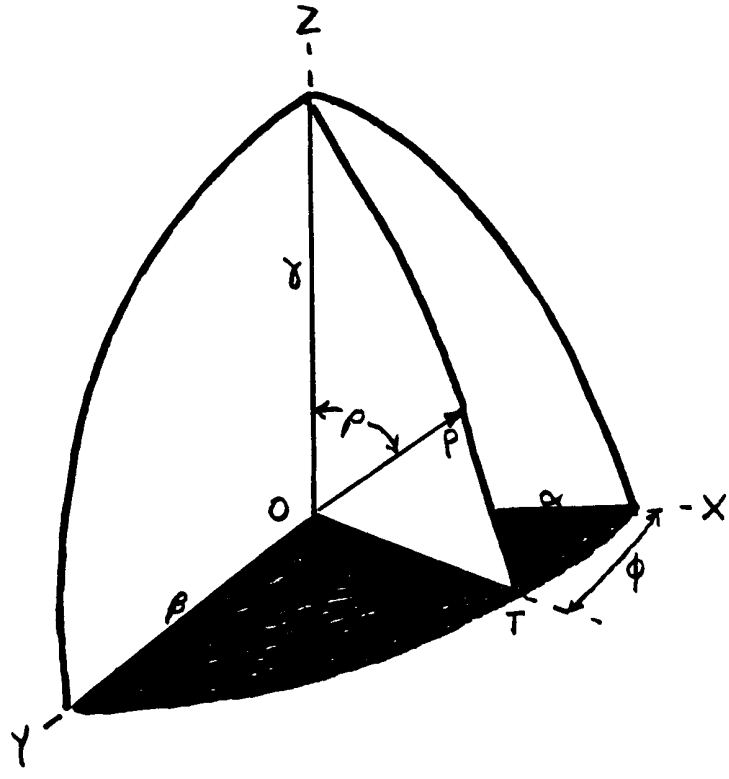

ρ = angle with principal axis Z

ϕ = angle between X and the unshaded plane containg OP and Z

Figure 14. The Biaxial Indicatrix (Bloss, 1961)

$$\alpha' = \frac{1}{\sqrt{\frac{\sin^2\rho\cos^2\phi}{\alpha^2} + \frac{\sin^2\rho\sin^2\phi}{\beta^2} + \frac{\cos^2\rho}{\gamma^2}}}$$

γ' = some formula, calculated by using the ϕ and ρ angles of the second extinction position close to γ

In contrast to biaxial minerals, uniaxial minerals have a single great circle, one optic axis and the cleavage normal. The intersection of this great circle and the plane representing the stage is the extinction position.

RESULTS

I calculated extinction angles and indices of refraction on (110) cleavage surfaces for nine pyroxenes. Some of the pyroxenes were given as $c \wedge Z$, and some were given as $c \wedge X$. The optical data and calculated results are given in Tables 1 and 2.

Two minerals, Jadeite and Aegirine, varied somewhat in the procedure, and it is with these two minerals that I'll describe the process. The first mineral, Jadeite, has the crystallographic axis b=Y, and $C \wedge Z = -30°$ to $-40°$ (Figure 15).

I first plotted the crystallographic directions X, Y and Z, and the two faces (110) and $(1\bar{1}0)$, (Jadeite shows typical pyroxene cleavage, distinct prismatic on (110) intersecting at 87° and 93°). Because the angle $C \wedge Z$ may be -30°, Z is plotted 30° from C on the ac plane. From the information given in Figure 1, we can see the angle $C \wedge Z$ is given as negative, which, in this case means that

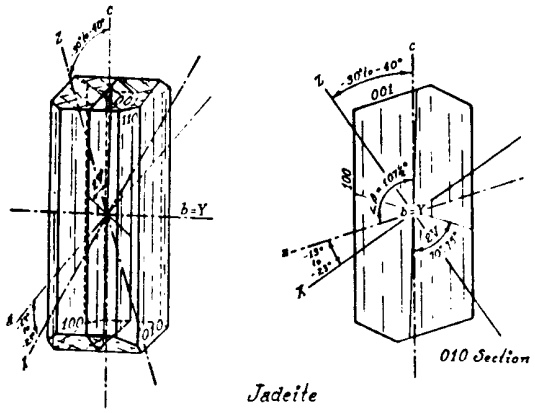

Jadeite

$n_\alpha = 1.654–1.665$*

$n_\beta = 1.659–1.674$

$n_\gamma = 1.667–1.688$

$n_\gamma - n_\alpha = 0.012–0.023$

Biaxial positive, $2V_z = 70° - 75°$

$b = Y$, $c \wedge Z = -30°$ to $-40°$, $a \wedge X = -13$ to $-23°$

$r > r$ moderate

Colorless in standard section

COMPOSITION. Jadeite composition commonly approaches the ideal $NaAl(SiO_3)_2$. It is the structural analog of diopside $CaMg(SiO_3)_2$, and an incomplete series probably exists where Na^{+}-Al^{3+} replaces Ca^{2+}-Mg^{2+}. The most significant impurity in jadeite seems to be Fe^{3+} as replacement for Al^{3+}, and a series may exist with aegirine $NaFe^{3+}(SiO_3)_2$. Omphacite $(Ca,Na)(Mg,Fe^{2+},Al,Fe^{3+})(SiO_3)_2$ appears as an intermediate member of the jadeite-diopside-aegirine complex.

Chemically, jadeite, $NaAl(SiO_3)_2$, is anhydrous analcite, $Na(AlSi_2O_6)\cdot H_2O$, and lies intermediate between albite, $Na(AlSi_3)O_2$, and nepheline, $Na(AlSi)O_4$. The latter three, however, are framework silicates.

* Ideal jadeite composition shows indices of refraction, birefringence, and $2V_z$ near the minimum values shown. These increase to somewhat indefinite upper limits with Fe^{3+}, Ca, Mg, and other impurities.

PHYSICAL PROPERTIES. H = 6. Sp. Gr. = 3.25–3.40. Color in hand sample, is white to light green or blue-green.

COLOR AND PLEOCHROISM. Jadeite is colorless to pale green in section or as fragments. Color seems related to Fe^{3+} substitution and may show distinct pleochroism in pale green and yellow.

FORM. Jadeite tends to occur as fine, fibrous aggregates, although coarse aggregates of anhedral granules to stubby euhedral crystals are also common.

CLEAVAGE. Jadeite shows typical pyroxene cleavages, distinct prismatic on {110} intersecting at 87° and 93°. Parting on {100} is reported.

BIREFRINGENCE. Jadeite tends to show low birefringence and low first-order colors in standard thin section. Ideal jadeite compositions show maximum birefringence near 0.012, in {010} sections, yielding no more than first-order yellow in standard section. Birefringence increases to yield low second-order colors toward diopside and aegirine compositions.

TWINNING. Fine multiple twinning on {100} and rarely on {001} is reported.

INTERFERENCE FIGURE. Jadeite is biaxial positive, with large $2V_z$ near 70°. Fragments on cleavages yield off-center figures without symmetry. {010} sections show flash figures, and other pinacoidal sections show off-center optic axis figures symmetrical about the optic plane. Few isochromes surround broad isogyres. Dispersion is moderately strong $r > r$ with possible inclined bisectrix dispersion. With increasing Fe^{3+} substitution, dispersion apparently reverses to $r > r$.

OPTICAL ORIENTATION. The optic plane of jadeite is {010}, $b = Y$. Z and X lie in {010} at angles to crystallographic directions $c \wedge Z = -30°$ to $-40°$ and $a \wedge X = -13°$ to $-23°$. Maximum extinction angle, seen in {010} sections, ranges from 30° to 40°. Extinction is parallel in {100} sections, symmetrical in basal sections, and somewhat less than maximum on cleavage fragments. Sign of elongation is positive (length-slow), as Z lies nearer elongation.

DISTINGUISHING FEATURES. Jadeite is distinguished from the fibrous, amphibole form of jade (nephrite) by pyroxene cleavage, higher refraction index, and larger extinction angles. Jadeite shows lowest refractive indices among the pyroxenes, except spodumene, and lower birefringence than other clino-

Figure 15. Example of Information Given for the Mineral Jadeite

this angle is measured towards the front of the crystal. If this angle is given as being on the front of the crystal, the point Z must be plotted towards the southern pole. X may now be placed 90° from Z in the ac plane (Figure 16).

Looking back at Figure 15, $2V_Z$ is set equal to 70°. This angle is positive and thus may be measured from Z, the acute bisectrix. Since Z bisects the optic axes 2V, the measurement is made 35° either side of Z (Z being the midpoint). According to Fresnel's law, two great circles which intersect both the face (110) and the face normal [110] may be plotted. The extinction position is the midpoint of these two intersection points on the microscope stage, or on the face (110) (Figure 17).

From this point measured 90° on the great circle representing the microscope stage, the second extinction position may be plotted.

To measure the extinction angle, count the number of degrees from the extinction position to the point where the microscope stage and the face $(1\bar{1}0)$ intersect (Figure 18).

The optic triangle may be plotted, keeping in mind the three great circles must intersect the crystallographic directions X, Y and Z. With the addition of the optic triangle, ϕ and ρ values may be measured for α' and γ'; the coordinates of α' are measured from X on the stereonet, and similarly, the coordinates of γ' are measured from Z (Figure 19).

The final step involves plugging this information into the equation given earlier (p.20):

$n_\alpha = 1.654$
$n_\beta = 1.659$ } from Figure 15
$n_\gamma = 1.667$

α'	γ'
$\phi = 39$	$\phi = 61$
$\rho = 87$	$\rho = 20$

} from the sterconet

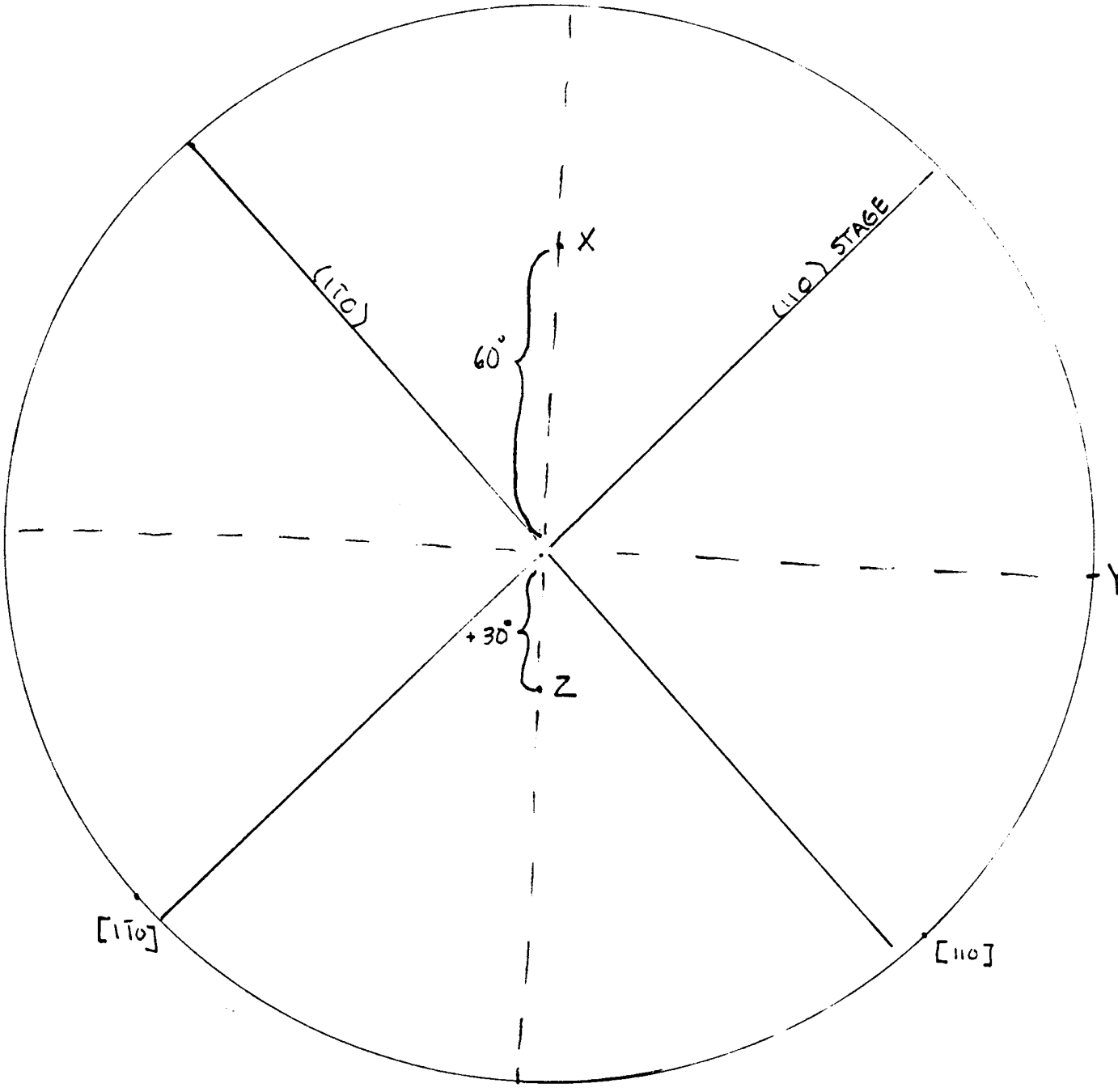

Figure 16. Placement of X, Y and Z for Jadeite and the Faces (110) and (1$\bar{1}$0)

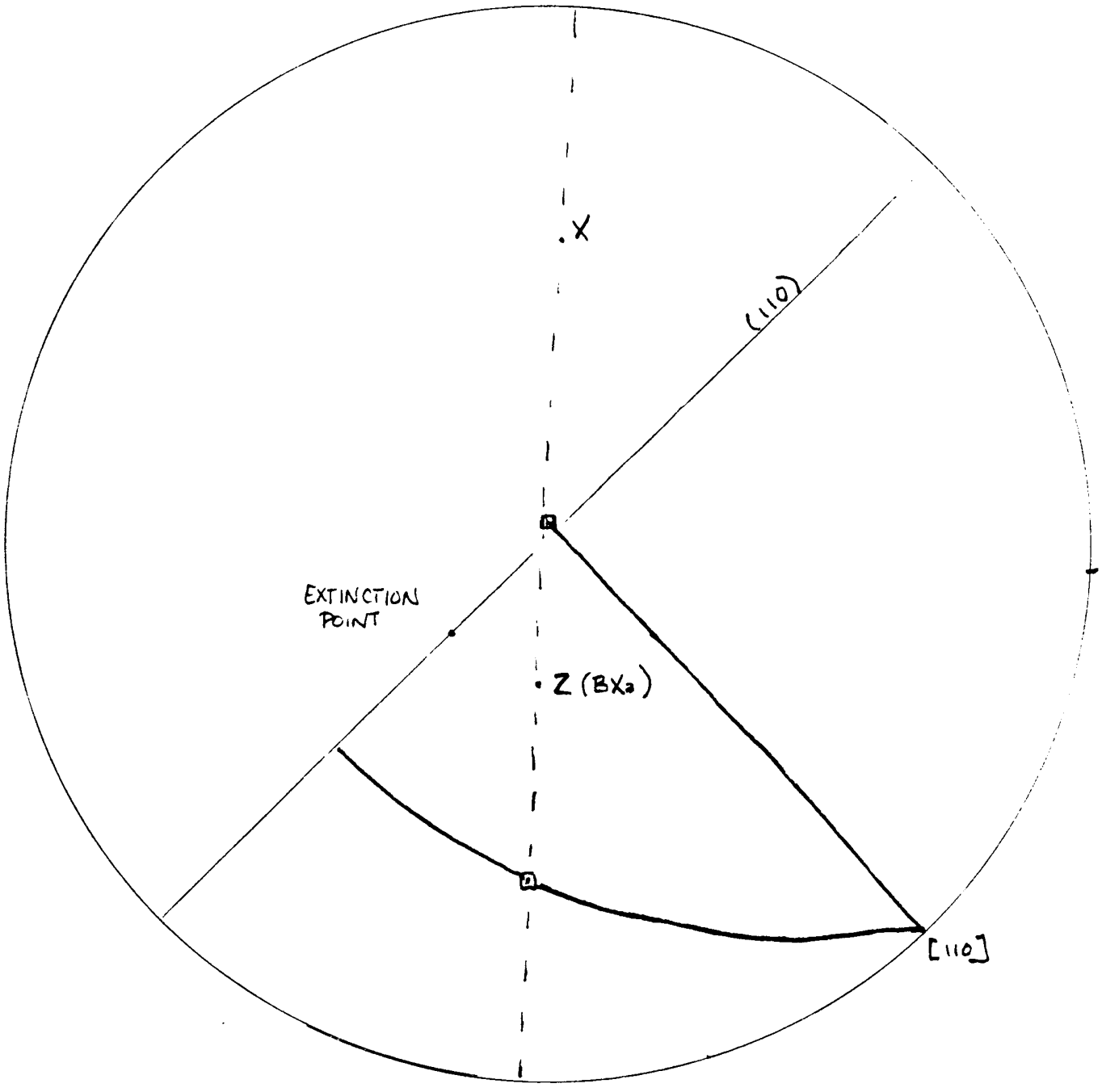

Figure 17. The Optic Axes and the Location of the Extinction Point for Jadeite on the Stereonet

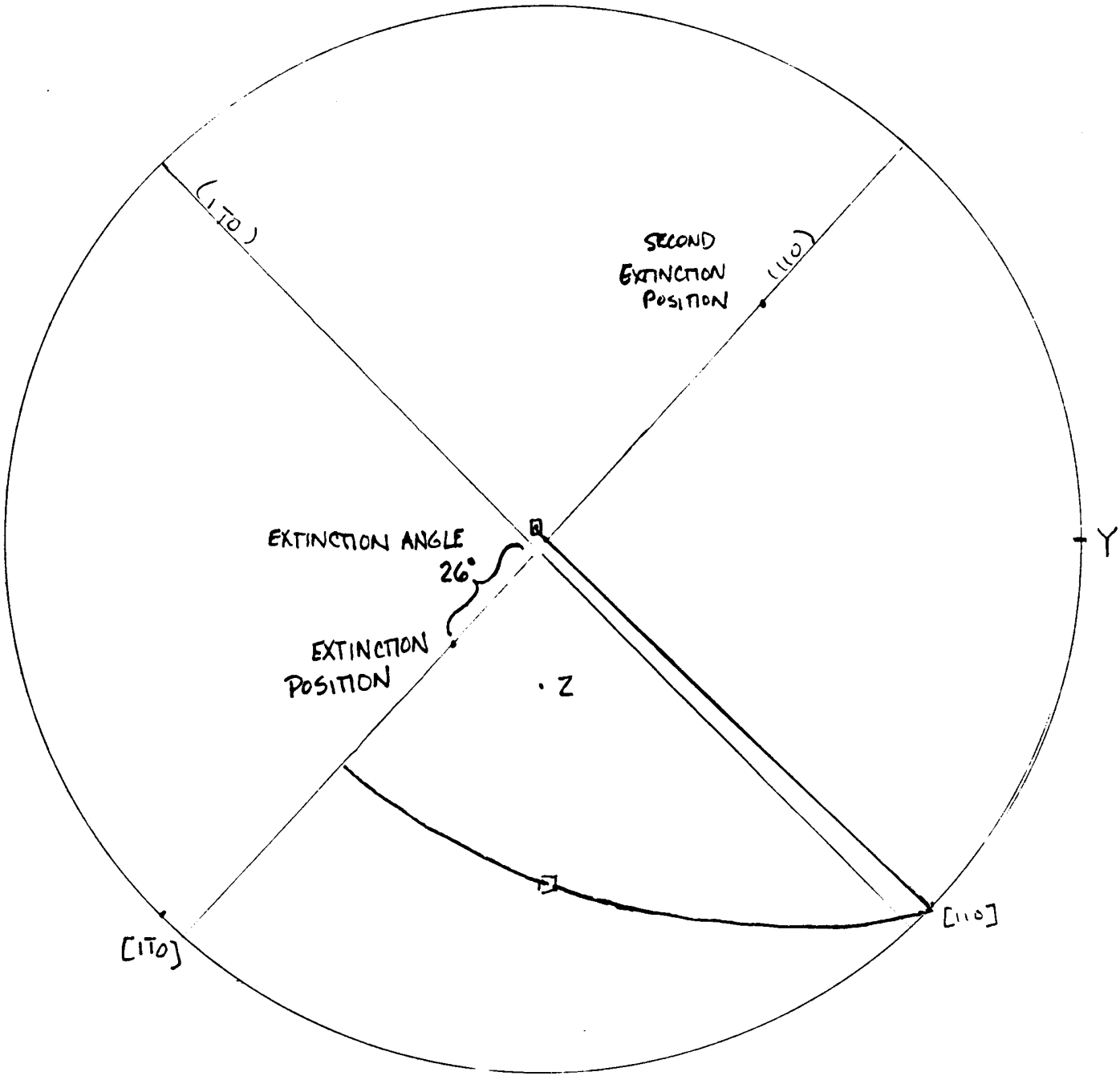

Figure 18. Plotting of the Second Measurement of the Extinction Angle with the Face (1$\bar{1}$0)

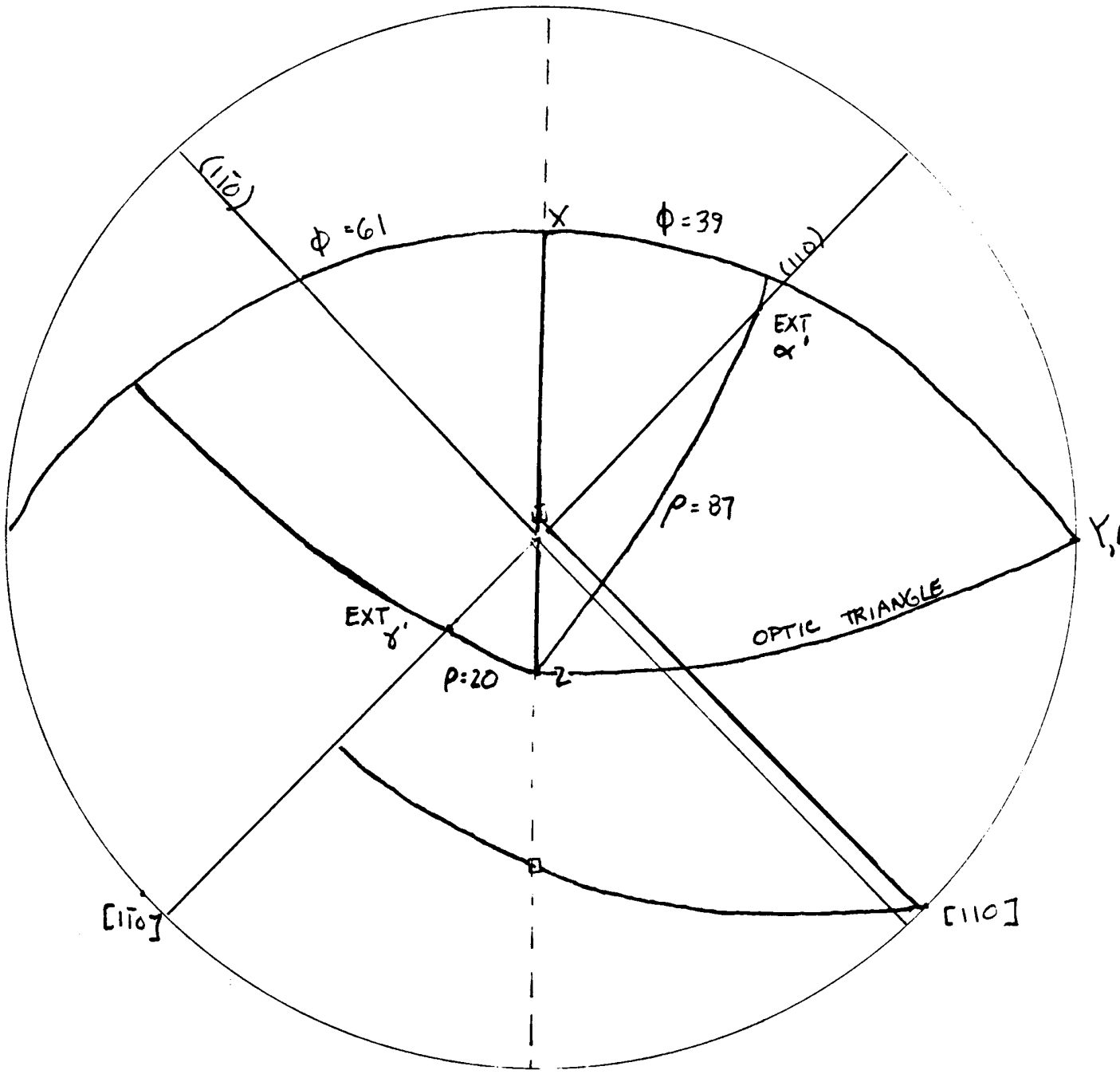

Figure 19. Direct Measurement of ϕ and ρ Coordinates of α' and γ', Completed Process for Jadeite

$$\gamma', \alpha' = \frac{1}{\sqrt{\frac{(\sin^2\rho)(\cos^2\phi)}{(n_\alpha)^2} + \frac{(\sin^2\rho)(\sin^2\phi)}{(n_\beta)^2} + \frac{(\cos^2\phi)}{(n_\gamma)^2}}}$$

$$\alpha' = \frac{1}{\sqrt{\frac{(\sin^2 87)(\cos^2 39)}{(1.654)^2} + \frac{(\sin^2 87)(\sin^2 39)}{(1.659)^2} + \frac{(\cos^2 87)}{(1.667)^2}}}$$

$$\alpha' = 1.656$$

$$\gamma' = \frac{1}{\sqrt{\frac{(\sin^2 20)(\cos^2 61)}{(1.654)^2} + \frac{(\sin^2 20)(\sin^2 61)}{(1.659)^2} + \frac{(\cos^2 20)}{(1.667)^2}}}$$

$$\gamma' = 1.666$$

Note: the values for α' and γ' are no greater than γ and no less than α.

This same process must be completed for the variation of C∧Z, 2V angle, and indices of refraction in the Jadeite Series (Figure 20).

In this example, the indices are taken from the variation:

$n_\alpha = 1.665$
$n_\beta = 1.674$
$n_\gamma = 1.688$

α': $\phi = 39$, $\rho = 86$ > from the stereonet < γ': $\phi = 66$, $\rho = 26$

$$\alpha' = \frac{1}{\sqrt{\frac{(\sin^2 86)(\cos^2 34)}{(1.665)^2} + \frac{(\sin^2 86)(\sin^2 34)}{(1.674)^2} + \frac{(\cos^2 86)}{(1.688)^2}}}$$

$$\alpha' = 1.668$$

$$\gamma' = \frac{1}{\sqrt{\frac{(\sin^2 26)(\cos^2 66)}{(1.665)^2} + \frac{(\sin^2 26)(\sin^2 66)}{(1.674)^2} + \frac{(\cos^2 26)}{(1.688)^2}}}$$

$$\gamma' = 1.685$$

Extinction Angle: =37°

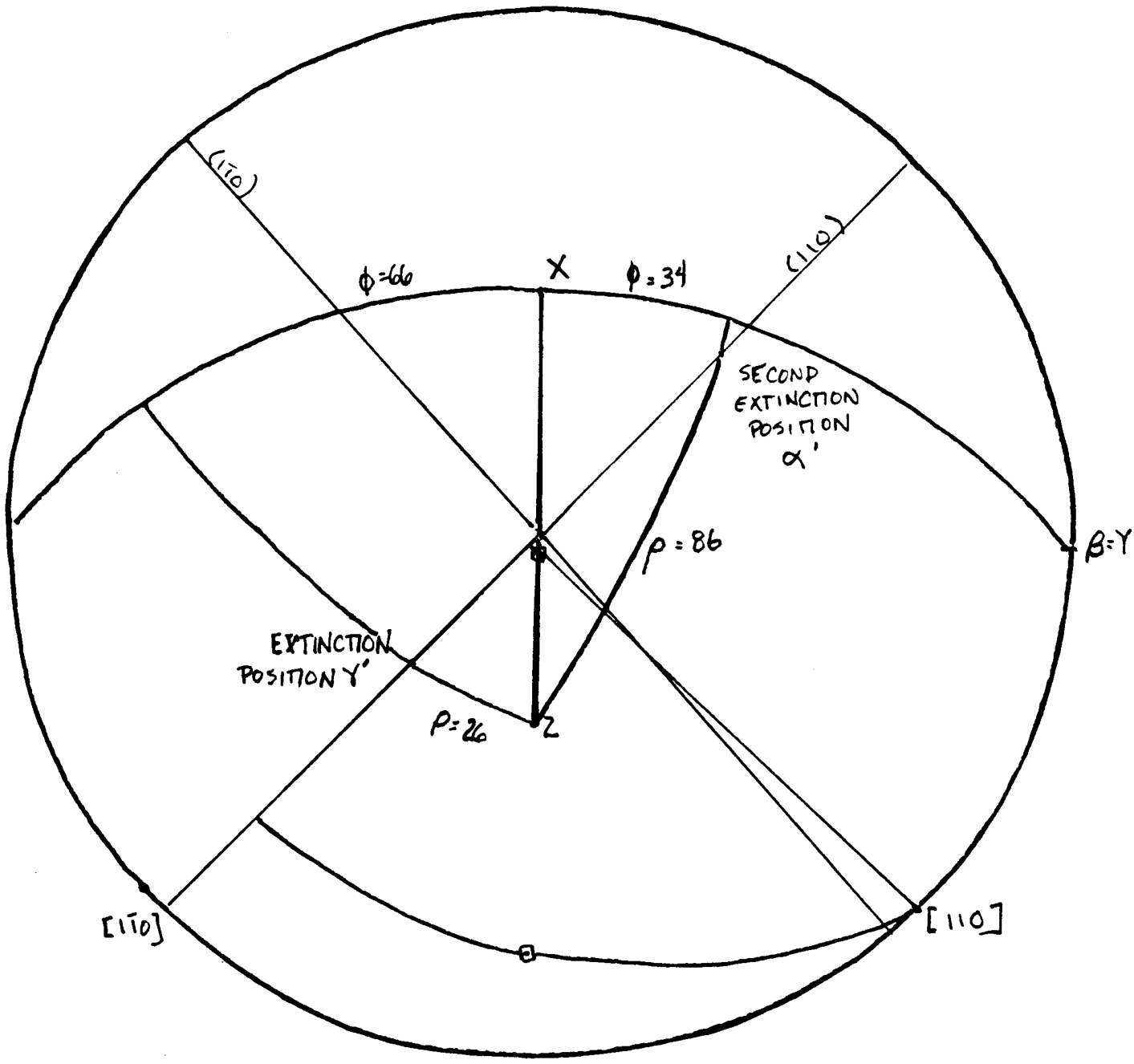

Figure 20. The Completed Process for the Variation of C∧Z, 2V Angle and Indices of Refraction for Jadeite

The same procedure is followed for the pyroxene Aegirine (Acmite). From the information in Figure 21 and Figure 22, we can see that the mineral is biaxial negative, $c \wedge X$ is -10° to +12°, $2V_X$ = 58°—90°, and the mineral is very different from Jadeite.

The main difference with Aegirine is that it is negative; therefore, X is taken to be the BXa, and X will bisect the optic axes. Since X is negative and measured to the back of the crystal, it is plotted north of the c crystallographic axis in the ac plane, and the 2V angle, which equals 58°, is bisected by X (Figure 23).

Figure 24A is the completion of the procedure: finding the extinction positions, the optic triangle, and the values of ϕ and ρ for α' and γ' in the same way as were located in Jadeite; the net yields the information:

$n_\alpha = 1.776$
$n_\beta = 1.820$
$n_\gamma = 1.836$

$$\alpha' = \frac{1}{\sqrt{\frac{(\sin^2 86)(\cos^2 6)}{(1.776)^2} + \frac{(\sin^2 86)(\sin^2 6)}{(1.820)^2} + \frac{(\cos^2 86)}{(1.836)^2}}}$$

$$\alpha' = 1.7763$$

α'	γ'
$\phi = 6$	$\phi = 90$
$\rho = 86$	$\rho = 43$

$$\gamma' = \frac{1}{\sqrt{\frac{(\sin^2 43)(\cos^2 90)}{(3.354)} + \frac{(\sin^2 43)(\sin^2 90)}{(3.312)} + \frac{(\cos^2 43)}{(3.371)}}}$$

$$\gamma' = 1.828$$

Again, as in Jadeite, we see a variation in $C \wedge X$, 2V angle, and indices of refraction (FIGURE 24B).

In Figure 24B we can see the extinction angle is calculated to be 12°. The values of α' and γ' are as follows:

α'	γ'
$\phi = 8$	$\phi = 85$
$\rho = 87$	$\rho = 42$

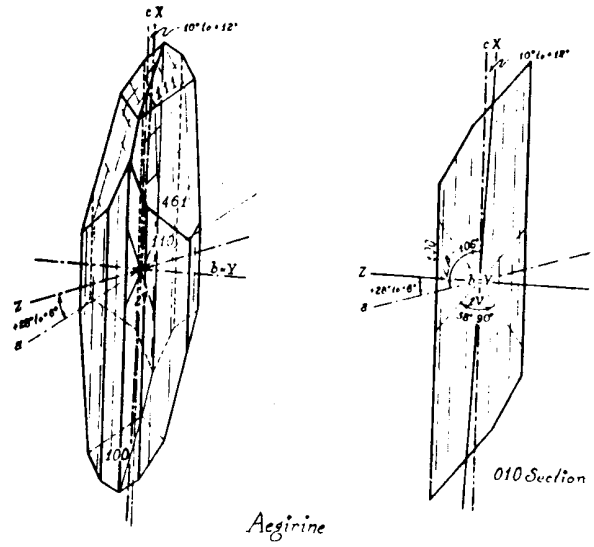

Aegirine (Acmite)

n_α = 1.776–1.722*

n_β = 1.820–1.742

n_γ = 1.836–1.758

$n_\gamma - n_\alpha$ = 0.060–0.036*

Biaxial negative

$2V_x$ = 58°–90°*

$b = Y$, $c \wedge X$ = −10° to +12°, $a \wedge Z$ = +28° to +6°

$r > v$ moderate to strong

Bright green to yellow-green in section, with pronounced pleochroism in deep green and yellow-green

$X > Y > Z$

Aegirine-Augite

n_α = 1.722–1.706

n_β = 1.742–1.710

n_γ = 1.758–1.730

$n_\gamma - n_\alpha$ = 0.036–0.030

Biaxial positive

$2V_z$ = 90–70

$b = Y$, $c \wedge X$ = +12 to +20, $a \wedge Z$ = +6 to −4

$r > v$ moderate to strong

Pale green to yellow-green in section, with weak pleochroism in pale yellow-green or brown-green

COMPOSITION. The ideal aegirine composition, $NaFe^{3+}(SiO_3)_2$, is analogous to diopside, $CaMg(SiO_3)_2$, with the replacement Na^+ and Fe^{3+} for Ca^{2+} and Mg^{2+}, and, indeed, aegirine-diopside represents a complete synthetic series (see Fig. 5-15). Natural compositions tend, however, to form essentially complete solid solution from $NaFe^{3+}(SiO_3)_2$ to augite compositions $(Ca,Na)(Mg,Fe^{2+},Fe^{3+},Al)[(Si,Al)O_3]_2$. Optical properties obviously become less definite toward the indefinite augite composition. Aegirine-augite is generally recognized as the intermediate member of the series, although its composition range is not generally agreed on. A change in

* See Fig. 5-14 for continuous optical variation with composition. Refractive indices, birefringence, and $2V_z$ increase toward aegirine.

Figure 21. Example of Information Given for Aegirine

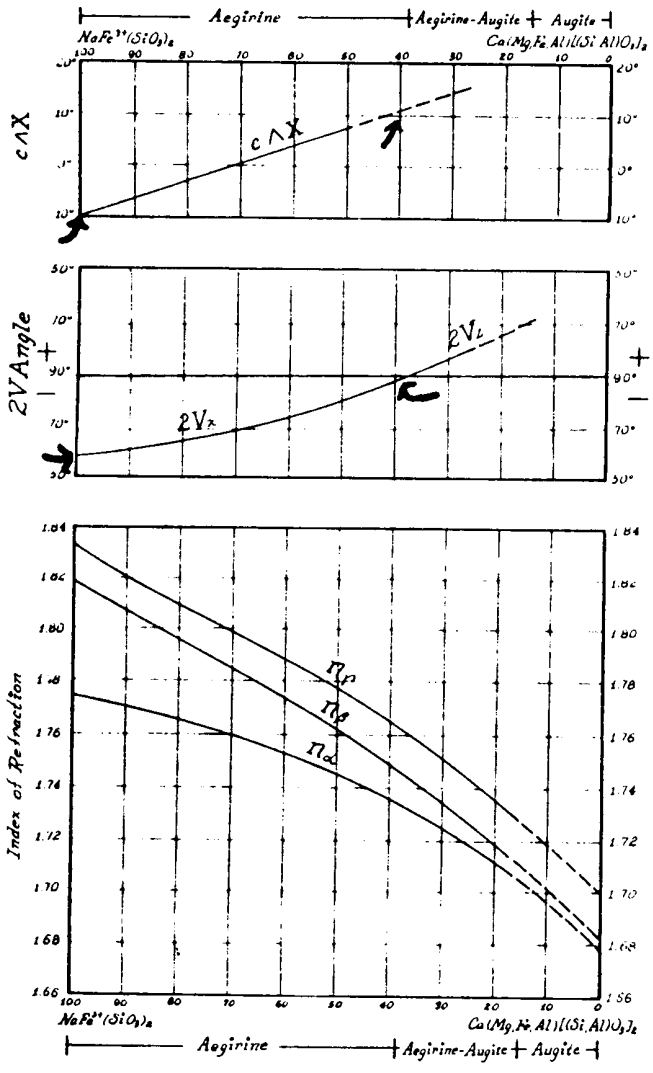

FIGURE 5-14. Variation of $c \wedge X$, $2V$ angle, and indices of refraction in the aegirine-augite series. (Data from Deer, Howie, and Zussman, 1962)

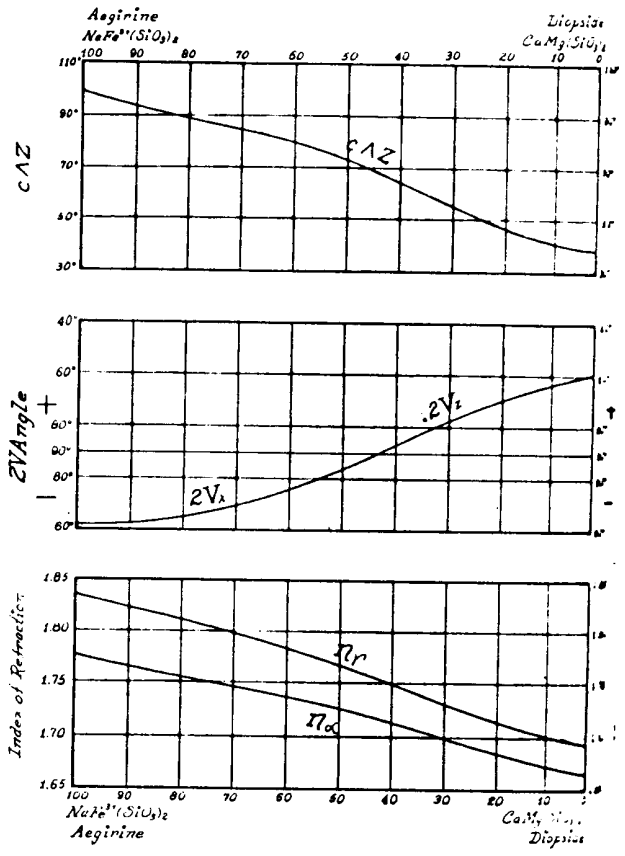

FIGURE 5-15. Variation of $c \wedge Z$, $2V$ angle, and refraction indices in the aegirine-diopside series.

optical sign at about Ae_{38} makes convenient optical division between aegirine and aegirine-augite and is adopted here. In natural compositions, the sign change appears over a narrow range due to indefinite composition and the augite to aegirine-augite boundary can only be arbitrarily defined in terms of the aegirine "molecule" at about Ae_{15}.

Aegirine	Ae_{100}–Ae_{38}
Aegirine-augite	Ae_{38}–Ae_{15}
Augite	Ae_{15}–Ae_0

Figure 22. Example of Information Given for Aegirine

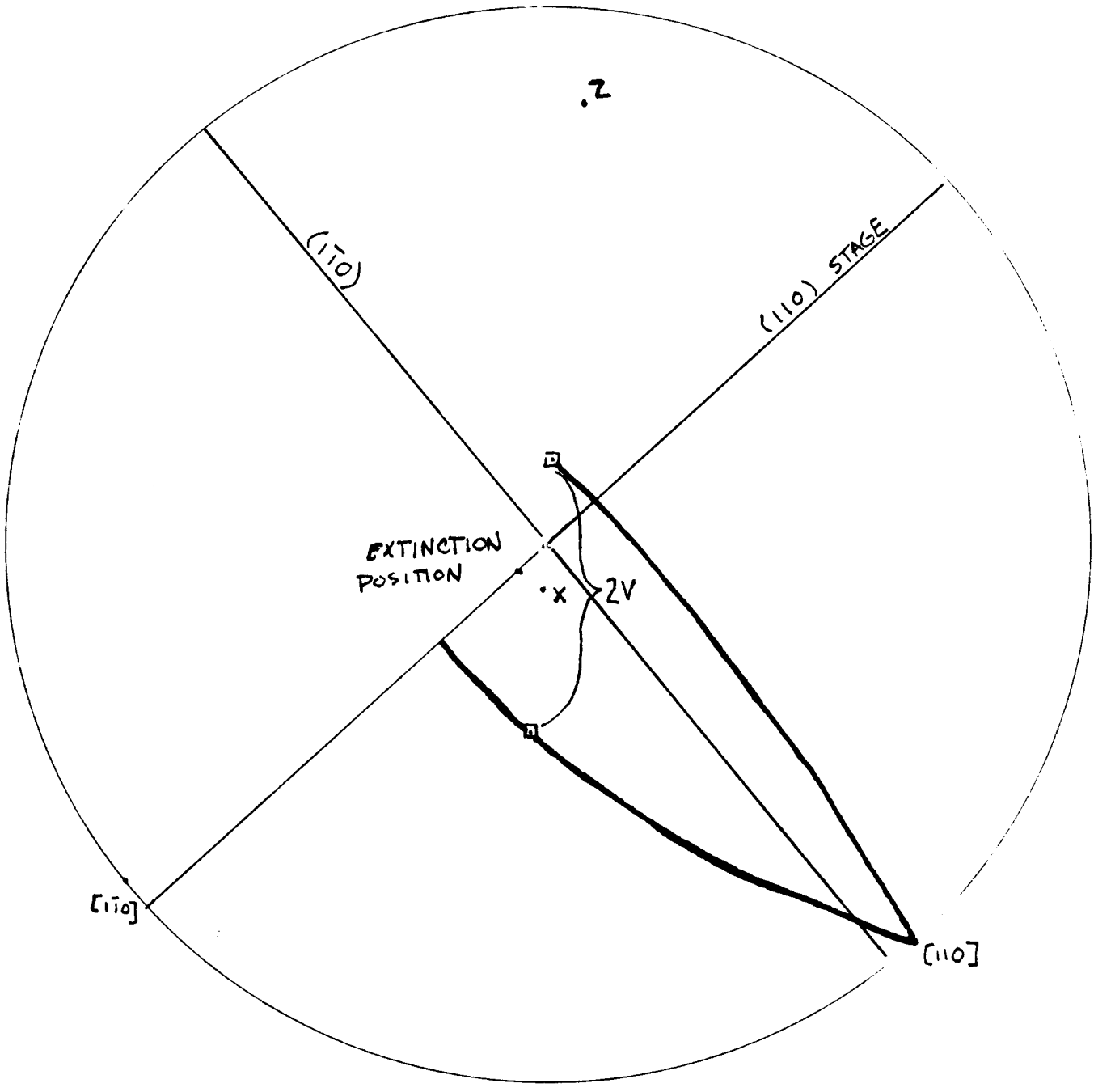

Figure 23. Plotting X, Y and Z Faces (110) and (110) and the Location of $2V_x$ for Aegirine , $c \wedge x = +10°$

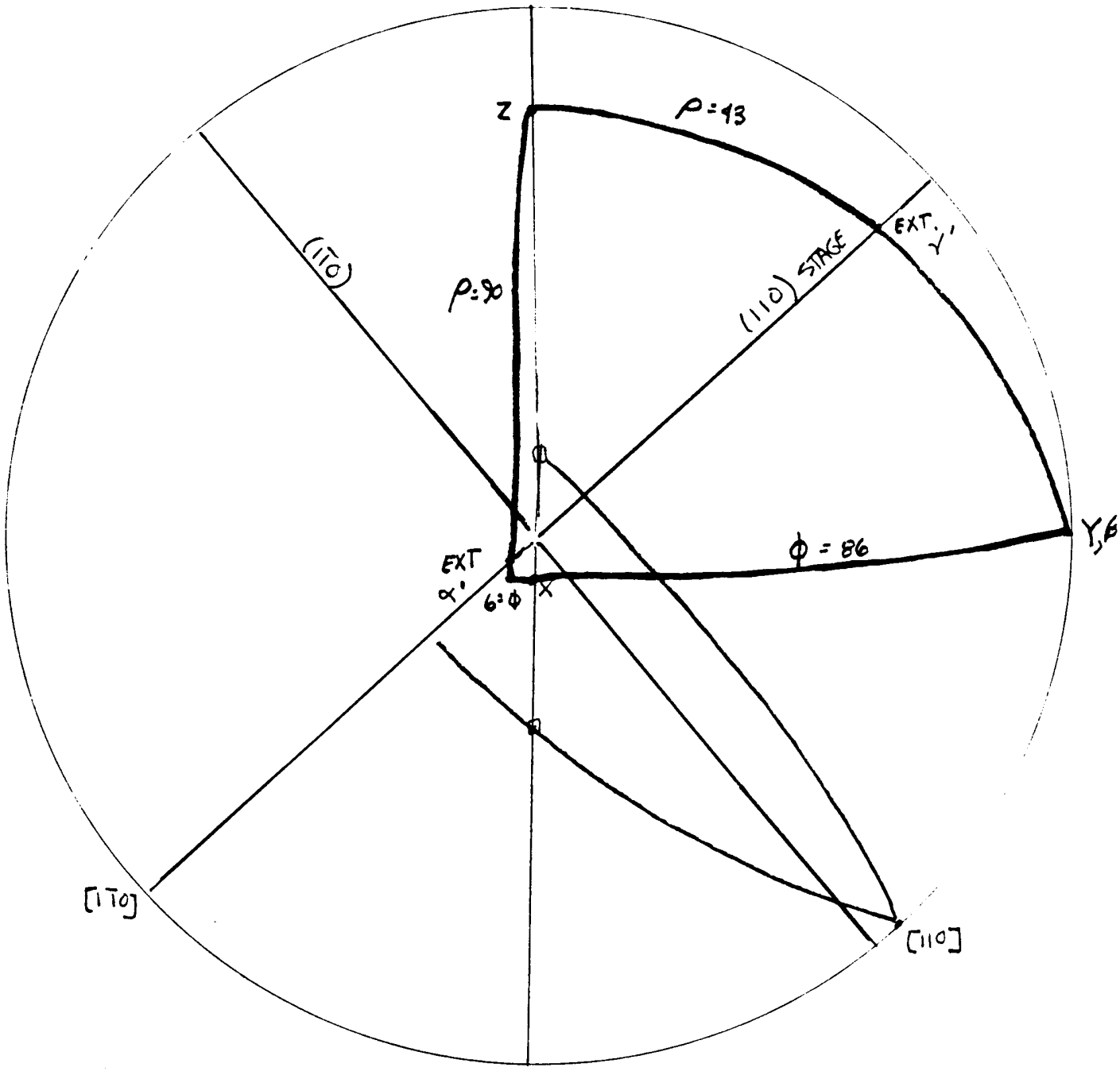

Figure 24A. Completion of the Procedure, $c \wedge x = 10^{\circ}$

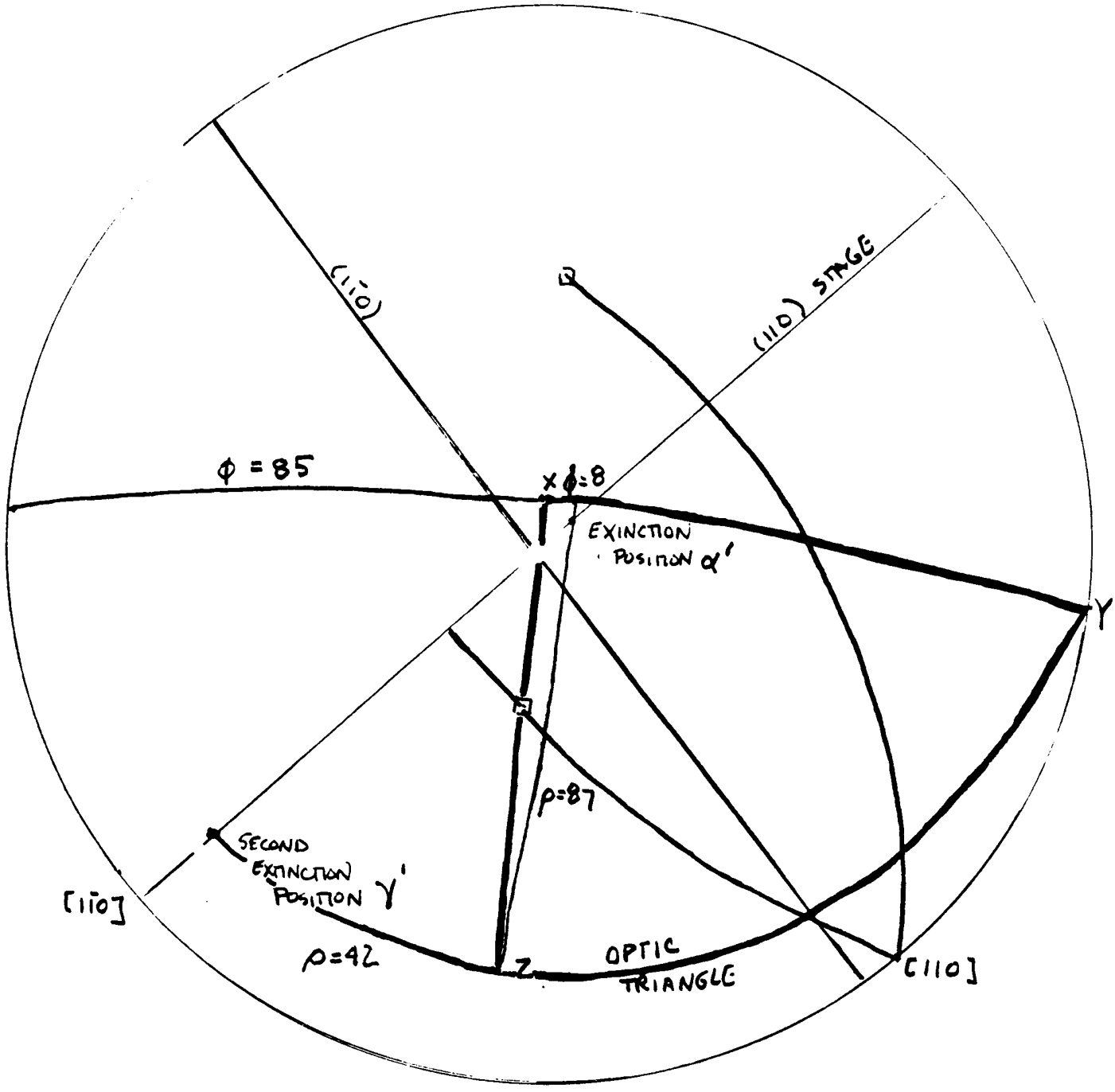

FIGURE 29 B. CAX = -12°

$$n_\alpha = 1.722$$
$$n_\beta = 1.742$$
$$n_\gamma = 1.758$$

Plugging these values into the equations, we may find the corresponding values of α' and γ'.

$$\alpha' = \frac{1}{\sqrt{\frac{(\sin^2 87)(\cos^2 8)}{(1.722)^2} + \frac{(\sin^2 87)(\sin^2 8)}{(1.742)^2} + \frac{(\cos^2 87)}{(1.758)^2}}}$$

$$\alpha' = 1.7223$$

$$\gamma' = \frac{1}{\sqrt{\frac{(\sin^2 42)(\cos^2 85)}{(1.722)^2} + \frac{(\sin^2 42)(\sin^2 85)}{(1.742)^2} + \frac{(\cos^2 42)}{(1.758)^2}}}$$

$$\gamma' = 1.751$$

TABLE 1 The extinction angles of nine pyroxene minerals as measured against the (1$\bar{1}$0) cleavage face

	Mineral	Extinction Angles
1	DIOPSIDE	33°
2	SALITE	37°
3	FERROSALITE	41.5°
4	HEDENBERGITE	42.5°
5	AEGIRINE (ACMITE)	8°, 12°
6	AEGIRINE-AUGITE	12°, 20.5°
7	JADEITE	26°, 37°
8	SPODUMENE	18°, 23.5°
9	OMPHACITE	31°, 47°

TABLE 2: The intermediate values α' and γ' of nine pyroxene minerals as calculated

	Mineral	α' and γ' values	
		α'	γ'
1	DIOPSIDE	$\phi = 35$ $\rho = 88$	$\phi = 63$ $\rho = 25$
2	SALITE	$\phi = 34$ $\rho = 86$	$\phi = 64$ $\rho = 28$
3	FERROSALITE	$\phi = 32$ $\rho = 86$	$\phi = 67$ $\rho = 30$
4	AEGIRINE (ACMITE)	8° extinction angle $\phi = 6$ $\rho = 86$ 12° extinction angle $\phi = 8$ $\rho = 87$	 $\phi = 90$ $\rho = 43$ $\phi = 85$ $\rho = 42$
5	AEGIRINE-AUGITE	12° extinction angle $\phi = 8$ $\rho = 87$ 20.5 extinction angle $\phi = 14$ $\rho = 86$	 $\phi = 85$ $\rho = 42$ $\phi = 81$ $\rho = 41$
6	HEDENBERGITE	$\phi = 30$ $\rho = 86.5$	$\phi = 65$ $\rho = 31$

TABLE 2 (continued)

		α'	γ'
7	JADEITE	26° extinction angle	
		$\phi = 39$	$\phi = 61$
		$\rho = 87$	$\rho = 20$
		37° extinction angle	
		$\phi = 34$	$\phi = 66$
		$\rho = 86$	$\rho = 26$
8	SPODUMENE	18° extinction angle	
		$\phi = 40$	$\phi = 55$
		$\rho = 89$	$\rho = 14$
		23.5° extinction angle	
		$\phi = 40$	$\phi = 59$
		$\rho = 88$	$\rho = 18$
9	OMPHACITE	31° extinction angle	
		$\phi = 36$	$\phi = 60$
		$\rho = 87$	$\rho = 24$
		47° extinction angle	
		$\phi = 28$	$\phi = 73$
		$\rho = 83$	$\rho = 32$

CONCLUSION

The intermediate values α' and γ' may be readily calculated by utilizing information gained from the stereonet. The process of calculating these prime values becomes essential when the index of refraction, at a given extinction position, cannot be directly measured. Normally the index is measurable when the grain itself is in the extinction position, and the indices exactly correspond in location to α, β and γ; unfortunately, the indices of refraction of these extinction positions rarely coincide with α, β, and γ and the calculation becomes necessary.

REFERENCES

BLOSS, F. Donald (1961). An Introduction to the Methods of Optical Crystallography, New York: Holt Rinehart and Winston, 231 pp.

HALLIMUND, A.F. (1970). The Polarizing Microscope, York: Vickers, p. 177.

HARTSHORNE, N.H. and STUART, A. (1964). Practical Optical Crystallography, New York: American Elsevier Company, pp. 256-263.

HARTSHORNE, N.H. and STUART, A. (1970). Crystals and the Polarizing Microscope, Fourth Ed., New York: American Elsevier Company, pp. 41-55, 285-290.

WAHLSTROM, Ernest E. (1969). Optical Crystallography, New York: John Wiley & Sons, pp. 10-19, 228, 445.

WINCHELL, Alexander N. (1951). Elements of Optical Mineralogy, New York: John Wiley & Sons, 551 pp.